CHALMERS

Testing of a new aftertreatment system for lean burn direct injected gasoline engines

Master of Science Thesis in the Master´s Programme Automotive Engineering

DANIEL IRESTÅHL
ANDREAS THULIN

Department of Applied Mechanics
Division of Combustion
CHALMERS UNIVERSITY OF TECHNOLOGY
Göteborg, Sweden 2011
Master's Thesis 2011:17

MASTER'S THESIS 2011:17

Testing of a new aftertreatment system for lean burn direct injected gasoline engines

Master of Science Thesis in the Master´s Programme Automotive Engineering

DANIEL IRESTÅHL, ANDREAS THULIN

Department of Applied Mechanics
Division of Combustion
CHALMERS UNIVERSITY OF TECHNOLOGY
Göteborg, Sweden 2011

Testing of a new aftertreatment system for lean burn direct injected gasoline engines

Master of Science Thesis in the Master´s Programme Automotive Engineering
DANIEL IRESTÅHL, ANDREAS THULIN

Master's Thesis 2011:17
ISSN 1652-8557
Department of Applied Mechanics
Division of Combustion
Chalmers University of Technology
SE-412 96 Göteborg
Sweden
Telephone: + 46 (0)31-772 1000

Chalmers Reproservice
Göteborg, Sweden 2011

Testing of a new aftertreatment system for lean burn direct injected gasoline engines

Master of Science Thesis in the Master´s Programme Automotive Engineering

DANIEL IRESTÅHL
ANDREAS THULIN
Department of Applied Mechanics
Division of Combustion
Chalmers University of Technology

ABSTRACT

A gasoline direct injected engine operating under lean conditions can offer a reduction in fuel consumption and a reduction of CO_2 emissions but meanwhile suffer from high levels of tailpipe NO_x emissions. A new way of reducing NO_x emissions in a lean burn gasoline engine is by using an ordinary three way catalyst (TWC) together with a selective catalytic reduction (SCR) catalyst, a passive SCR concept. The basic idea of this concept is that ammonia could be formed over the TWC by operating the engine rich during short amounts of time. The produced ammonia can then be stored in the SCR catalyst further down the exhaust system. When the engine switches into lean operation the stored ammonia is then used to reduce the engine out NO_x emissions over the SCR catalyst.

The purpose of this master thesis was to investigate if the passive SCR concept is a possible exhaust aftertreatment system to reduce tailpipe NO_x emissions for gasoline lean burn engines. This project was performed in an engine test cell at Chalmers University of Technology and was carried out experimentally. The intention was to investigate how much ammonia that could be formed over the TWC, if ammonia were stored on the SCR catalyst bed and if NO_x was reduced over the SCR catalyst.

To conclude, the passive SCR concept is a possible exhaust aftertreatment system. Ammonia was formed over the TWC by operating rich. It was noticed that lambda, engine load and rich cycle duration affected the amount of ammonia formed at steady state conditions. The major drawback was that when ammonia was formed increased concentrations of CO was detected post the TWC. As for the SCR catalyst it was concluded that it was temperature dependent. It was noticed that there was a tradeoff between ammonia storage capacity and NO_x reduction efficiency. Increased temperature promoted NO_x reduction efficiency and demoted ammonia storage capacity.

Key words: Ammonia, NH_3, NO_x, TWC, Three way catalyst, SCR, Lean burn, SIDI, Emissions, Exhaust aftertreatment systems.

Table of Contents

ABSTRACT I
TABLE OF CONTENTS III
PREFACE V

NOTATIONS VI
List of figures VIII
List of tables IX

1 INTRODUCTION 1
1.1 Background 1
1.2 Purpose 2
1.3 Objective 2
1.4 Scope 2

2 SPARK IGNITED DIRECT INJECTED GASOLINE ENGINE 3
2.1 Homogeneous charge 3
2.2 Stratified charge 4
2.3 Lean operation 4

3 EMISSIONS FROM SI GASOLINE ENGINES 6
3.1 Emissions formation overview 6
3.2 Formation of NO 7
3.3 Formation of CO 7
3.4 Formation of HC 8
3.5 Emissions of lean burn engines 8

4 CATALYTIC CONVERTERS 9
4.1 Introduction to catalytic converters 9
4.2 Three Way Catalyst 10
4.3 Lean NO_x Trap 11
4.4 Selective Catalytic Reduction 11

5 PASSIVE SCR 13

6 AMMONIA FORMATION FACTORS 11
6.1 Sulfur level 14
6.2 Composition of a TWC 14
6.3 Rich cycle duration 16
6.4 Air-to-fuel ratio 16

7 EXPERIMENTS 18
7.1 Engine and related systems 18
7.1.1 Three way catalysts 19
7.1.2 Selective catalytic reduction catalysts 19
7.2 Experimental test setup 20
7.2.1 Hardware 20

7.2.2 Software 24
7.3 Experiment plan 25
7.3.1 Ammonia formation steady state 25
7.3.2 Ammonia formation at lambda cycling 26
7.3.3 Depletion of OSC 26
7.3.4 Ammonia storage capacity and NO_x reduction efficiency 27

8 RESULTS 28
8.1 Ammonia formation steady state 28
8.2 Ammonia formation at lambda cycling 35
8.3 Depletion of OSC 38
8.4 Ammonia storage capacity and NO_x reduction efficiency 39

9 CONCLUSIONS 44

10 FUTURE WORK AND RECOMMENDATIONS 45

11 REFERENCES 46

APPENDIX A - CALCULATIONS I

Preface

This report concludes our master thesis and was carried out from 10th of January until 27th of May 2011 on behalf of Volvo Car Corporation in co-operation with Haldor Topsøe A/S and Chalmers University of Technology. It is the degree project for our Master of Science in Mechanical Engineering at Chalmers University of Technology. All work and experimental tests have been carried out in the engine laboratory at the Department of Applied Mechanics, Division of Combustion at Chalmers University of Technology.

First and foremost we would like to thank our supervisor Daniel Dahl and our examiner professor Ingmar Denbratt at Chalmers University of Technology for their assistance, guidance and support during the project. We would like to thank Mats Laurell and Andreas Berntsson at Volvo Car Corporation for their assistance with our questions. At the same time we would like to thank Volvo Car Corporation for providing us with an engine, catalysts, fuel and measurement equipment. We would also like to thank Pär Gabrielsson and Andreas Vressner at Haldor Topsøe A/S for their co-operation and involvement in the project and the lending of their FTIR equipment and SCR catalyst.

Finally, we would thank the laboratory staff at Chalmers for their assistance in the engine test cell.

Daniel Ireståhl
Andreas Thulin

Göteborg 27th of May, 2011

Notations

Abbreviations and acronyms

AFR	Air to Fuel Ratio
AM	Amplitude Modulation
BaO	Chemical denomination of barium oxide
BMEP	Brake Mean Effective Pressure
BSFC	Brake Specific Fuel Consumption
CAD	Crank Angle Degrees
CCC	Closed Coupled Catalysts
Ce	Chemical denomination of cerium
CIDI	Compression Ignited Direct Injected
CO	Chemical denomination of carbon monoxide
CO_2	Chemical denomination of carbon dioxide
Cu	Chemical denomination of copper
DAQ	Data Acquisition
DI	Direct Injected
ECU	Engine Control Unit
Fe	Chemical denomination of iron
FTIR	Fourier Transform InfraRed
GDI	Gasoline Direct Injected
H_2	Chemical denomination of hydrogen
H_2O	Chemical denomination of water
HC	Chemical denomination of hydrocarbon
IMEP	Indicated Mean Effective Pressure
Lean	Excessive air in the combustion mixture
LNT	Lean NO_x Trap
N_2	Chemical denomination of diatomic nitrogen
NEDC	New European Driving Cycle
NH_3	Chemical denomination of ammonia
NO	Chemical denomination of nitrogen monoxide
NO_2	Chemical denomination of nitrogen dioxide
NO_x	Chemical denomination of nitrogen oxides, the sum of NO + NO_2
O_2	Chemical denomination of oxygen
OSC	Oxygen Storage Capacity
Pd	Chemical denomination of palladium

PFI	Port Fuel Injection
PGM	Platinum Group Metals
PM	Particulate Matter
Pt	Chemical denomination of platinum
Rh	Chemical denomination of rhodium
Rich	Excessive fuel in the combustion mixture
RPM	Revolutions Per Minute
SCR	Selective Catalytic Reduction
SI6	Short Inline 6
SIDI	Spark Ignited Direct Injected
SO_2	Chemical denomination of sulfur dioxide
TWC	Three Way Catalyst
UDS	Urea Dosing System
UFC	Under Floor Catalyst
VCC	Volvo Car Corporation
VE	Volumetric Efficiency

Units

°C	Degree Celsius
bar	Pressure
C_p	Specific heat at constant pressure
C_v	Specific heat at constant volume
K	Degree Kelvin
m	Mass
$\dot{m}$	Mass flow
M	Molar mass
n	Mole
ppm	Parts Per Million
r_c	Compression ratio
η	Efficiency
λ	Lambda

List of figures

Figure 1. Engine speed-load map at different operating modes of an SIDI [1]. 3
Figure 2. Fuel consumption and specific NO_x as a function of BMEP for homogeneous and stratified charged for a SIDI engine [2]. 4
Figure 3. Emissions from SI gasoline engines at different AFR [4]. 6
Figure 4. Different monolithic substrate designs, a) honeycomb, b) laminar with straight layers, c) laminar with wavy layers [8]. 9
Figure 5. Conceptual layout of a LNT aftertreatment system. 11
Figure 6. Conceptual layout of a SCR aftertreatment system. 12
Figure 7. Conceptual layout of a passive SCR aftertreatment system. 13
Figure 8. Effect of low sulfur gasoline upon NH_3 and N_2O [18]. 14
Figure 9. NH_3 formation (dotted line) due to TWC compositions [13]. 15
Figure 10. NH_3 formation of Pd only (left) and Pd/Pt/Rh TWC (right) [19]. 15
Figure 11. NO_x, NH_3 and N_2O formation as a function of cycle duration for a LNT [20]. 16
Figure 12. AFR sweep test for NH_3 formation on a TWC [22]. 17
Figure 13. Overview of the modified exhaust system. 18
Figure 14. Elliptic TWC 1 to the left and circular TWC 1 to the right. 19
Figure 15. VCC SCR to the left and Haldor Topsøe A/S SCR to the right. 20
Figure 16. Location of added sockets to the TWC and first part of the exhaust system. 21
Figure 17. ETAS Lambda Meter LA4, charge amplifier, AM-Module, analogue input module and AVL IndiMaster. 22
Figure 18. Emission analyzer equipment. 23
Figure 19. Overview of added sockets to the SCR and the second part of the exhaust system. 24
Figure 20. NH_3 formation for TWC 1 at 800rpm and at (a) 0.5bar BMEP, (b) 3bar BMEP, (c) 7bar BMEP. 29
Figure 21. NH_3 formation for TWC 1 at 1500rpm and at (a) 0.5bar BMEP, (b) 3bar BMEP, (c) 7bar BMEP. 29
Figure 22. NH_3 formation for TWC 1 at 2000rpm and at (a) 0.5bar BMEP, (b) 3bar BMEP, (c) 7bar BMEP. 29
Figure 23. NH_3 formation for TWC 1 at 3000rpm and at (a) 0.5bar BMEP, (b) 3bar BMEP, (c) 7bar BMEP. 30
Figure 24. NH3 formation for TWC 2 at 800rpm and at (a) 0.5bar BMEP, (b) 3bar BMEP, (c) 7bar BMEP. 30
Figure 25. NH_3 formation for TWC 2 at 1500rpm and at (a) 0.5bar BMEP, (b) 3bar BMEP, (c) 7bar BMEP. 31
Figure 26. NH_3 formation for TWC 2 at 2000rpm and at (a) 0.5bar BMEP, (b) 3bar BMEP, (c) 7bar BMEP. 31
Figure 27. NH_3 formation for TWC 2 at 3000rpm and at (a) 0.5bar BMEP, (b) 3bar BMEP, (c) 7bar BMEP. 31
Figure 28. 800rpm steady state NH_3 formation. 32

Figure 29. 1500rpm steady state NH_3 formation. 32
Figure 30. 2000rpm steady state NH_3 formation. 32
Figure 31. 3000rpm steady state NH_3 formation. 32
Figure 32. NH_3 formation for TWC1 at a) 0.5bar BMEP, b) 3bar BMEP c) 7bar BMEP. 33
Figure 33. NH_3 formation for TWC2 at a) 0.5bar BMEP, b) 3bar BMEP c) 7bar BMEP. 33
Figure 34. NH_3 formation for TWC1 as a function of engine out NO_x and CO. 34
Figure 35. NH_3 formation for TWC2 as a function of engine out NO_x and CO. 34
Figure 36. Lambda cycling 0.99-1.01 at 1500rpm 3bar BMEP. 35
Figure 37. Lambda cycling 0.98-1.02 at 1500rpm 3bar BMEP. 36
Figure 38. Lambda cycling 0.95-1.05 at 1500rpm 3bar BMEP. 37
Figure 39. OSC depletion test at 1500rpm and 3bar BMEP. 38
Figure 40. NH_3 storage capacity test and NO_x reduction at 1500rpm and 3bar BMEP for SCR 1. 39
Figure 41. NH_3 storage capacity test and NO_x reduction at 1500rpm and 3bar BMEP for SCR 2. 40
Figure 42. SCR NH_3 storage capacity for different brick temperatures. 40
Figure 43. NO_x reduction efficiency for SCR 1 at 1500rpm and 3bar BMEP. 41
Figure 44. NO_x reduction efficiency for SCR 2 at 1500rpm and 3 BMEP. 42
Figure 45. SCR NO_x reduction efficiency at 1500rpm and 3bar BMEP. 42
Figure 46. Lambda cycling at 0.1Hz, 1500rpm and 3bar BMEP. 43

List of tables

Table 1. Technical specification of the experimentally tested engine. 18
Table 2. Description of the modified exhaust system. 19
Table 3. Properties of the TWCs. 19
Table 4. Properties of the SCRs. 20
Table 5. Description of added sockets to the TWC and first part of the exhaust system. 20
Table 6. Description of added sockets to the SCR catalyst and second part of the exhaust system. 23
Table 7. Test matrix of the NH_3 formation test. 25
Table 8. Test matrix of the lambda cycling test. 26

1 Introduction

An introduction to the project is described in this chapter.

1.1 Background

The fossil fuel consumption of propulsion vehicles becomes more and more important due to the emissions of carbon dioxide (CO_2) and their direct relation to global warming. A decrease in fuel consumption will both reduce the environmental stress of our planet and save money for the consumer. Advanced combustion technologies have improved combustion properties which has reduced both fuel consumption and emissions during the past decades. Stricter regulations of pollutant emissions drive automotive manufactures to develop more fuel efficient and less pollutant engines and the trend will continue. Different techniques exist in order to reduce fuel consumption, but the main problem is to reduce both fuel consumption and emissions.

Internal combustions engines developed for passenger cars today are mainly designed for three kinds of fuels: gasoline, diesel and alcohols. Diesel engines have low fuel consumption since they operate at excessive air with no throttle and with high compression ratio. Their main drawback is increased emissions of nitrogen oxides (NO_x) and particulate matter (PM), which requires an aftertreatment system. A modern gasoline or alcohol engine operates at a stoichiometric air-to-fuel ratio (AFR) and uses a three way catalyst (TWC) to reduce emissions. This is a proven technique, however operating at stoichiometric conditions requires throttling of air which is a problem for further improvements.

A gasoline direct injected (GDI) engine operating under lean conditions can offer a reduction in fuel consumption and a reduction of CO_2 emissions, but meanwhile suffers from high tailpipe NO_x emissions. The most common way today to deal with NO_x emissions is by using a lean NO_x trap (LNT) as an aftertreatment system. An LNT has the ability to store the engine out NO_x during lean operation. When the LNT is almost filled it requires purging of the stored NO_x emissions. This is done by operating the engine rich and thereby the stored NO_x is reduced to diatomic nitrogen (N_2). An LNT has some major drawbacks such as high platinum group metal (PGM) needs, which adds to the manufacturing cost of the catalyst, poor thermal durability, sulfur poisoning and requires active sulfur dioxide (SO_2) regeneration.

To handle the NO_x emissions on heavy trucks propelled with diesel engines, an alternative aftertreatment system is used. This is a selective catalytic reduction (SCR) catalyst which reduces NO_x with the help of a reducing agent such as urea. Urea is injected from a separate tank into the exhaust gas stream which reduces NO_x once it reaches the SCR catalytic bed. The main drawback with this technology is that an additional tank containing urea and an injection system are needed which adds to the costs and complexity of the aftertreatment system.

A new way of reducing NO_x emissions in a lean burn gasoline engine is by using an ordinary TWC together with a SCR catalyst, a passive SCR concept. The basic idea of this concept is that ammonia (NH_3) could be formed over the TWC by operating the engine rich during short amounts of time. The produced NH_3 can then be stored on the SCR catalyst further down the exhaust system. When the engine switch into lean operation the stored NH_3 is used to reduce the NO_x emissions over the SCR catalyst. By using this type of system an additional urea system is not required.

1.2 Purpose

The purpose of this master thesis was to investigate if the passive SCR concept is a possible exhaust aftertreatment system to reduce tailpipe NO_x emissions for gasoline spark ignited direct injected (SIDI) lean burn engines.

1.3 Objective

The objective of this master thesis was to investigate how much NH_3 that could be formed over two separate TWCs with different PGM composition by operating the engine rich. In the subsequent test the NH_3 storage capacity and the NO_x reduction efficiency of the two SCRs was investigated.

The following questions were investigated and analyzed:

- How much NH_3 can be formed over a TWC at different operating conditions?
- How much NH_3 can be stored on the SCR catalyst bed?
- What is the NO_x reduction efficiency of the SCR?
- Is the passive SCR concept a possible exhaust aftertreatment system to reduce NO_x for gasoline lean burn engines?

1.4 Scope

This master thesis was performed in an engine test cell at Chalmers University of Technology and was carried out experimentally. The time in the engine test cell was limited to two months and therefore some contributing factors to NH_3 formation were not considered due to its complexity and time limitation.

The selected parameters to investigate regarding NH_3 formation were engine speed (RPM), brake mean effective pressure (BMEP), lambda (λ), TWC composition and rich cycle duration. The NH_3 formation depends on several operating parameters, though earlier research has showed the main parameter affecting the NH_3 formation is the mixture composition. Other possible and relevant parameters were investigated by literature studies.

The experiments on NH_3 storage capacity and NO_x reduction efficiency of the SCR catalysts were performed at a fixed load and engine speed with varied brick temperature.

The tests were carried out on a SIDI gasoline engine operating in homogenous mode. No cold starts and no transient engine speeds or loads were investigated. The tests were all experimental and no simulation was carried out in this master thesis.

2 Spark ignited direct injected gasoline engine

The brake specific fuel consumption (BSFC) of a diesel compression ignited direct injected (CIDI) engine is lower compared to a gasoline port fuel injected (PFI) engine, mainly due to higher compression ratio and unthrottled operation. The diesel engine has increased emissions of PM, NO_x and higher noise level together with decreased engine speed range compared to a SI engine [1]. During the past, attempts have been made to develop an engine which combines the benefits from both CIDI and SI engines. The goal has been a specific power output of an SI engine and the high efficiency of a CIDI engine at low loads. The SIDI engine has been developed during the past decades and a number of different concepts have been investigated in order to reduce BSFC. The SIDI engine has the injection of fuel directly into the cylinder generating a mixture which is ignitable at the spark plug. The difficulty with SIDI engines is the controllability of the fuel injection system, though the advantages of SIDI are attributed to the flexibility of the fuel system [2]. In general the SIDI engine can be divided into two different operating modes: homogeneous charge and stratified charge. In Figure 1 the operating range for each mode can be seen in a load-engine speed map.

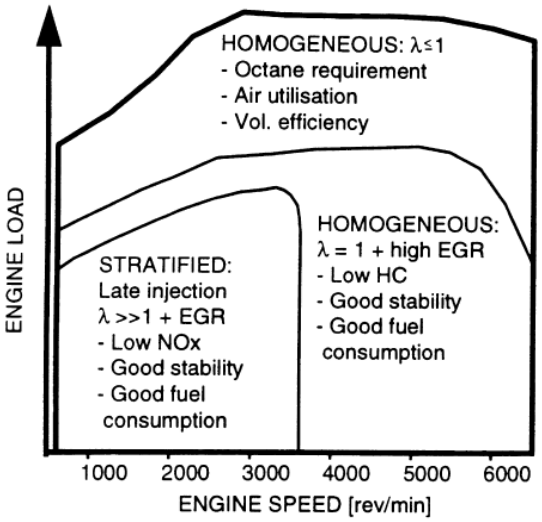

Figure 1. Engine speed-load map at different operating modes of an SIDI[1].

2.1 Homogeneous charge

The homogeneous charge mode has the injection of fuel during the intake stroke. The fuel mixes with the incoming air and forms a homogeneous mixture. The homogeneous operation is similar to regular PFI operation except the fuel is injected at high pressure directly into the combustion chamber instead of in the port. This limits the injection period to approximately 180 crank angle degrees (CAD). To overcome the decreased injection period the injection pressure is increased which promotes mixture formation due to increased turbulence. The target mixture composition is achieved by throttling the intake air and supplying the correct amount of fuel during the injection. The gas mixture is ideally pre-mixed and homogenous in composition anywhere in the cylinder when ignition occurs. Target mixture composition for homogenous mode is usually $\lambda = 1$ at part load and slightly richer at higher loads to achieve maximum performance and gain benefits of the cooling effect of the fuel [1], [3]. Compared to regular PFI SI engines the benefits of direct injected

(DI) are increased volumetric efficiency (VE), increased power and reduced hydrocarbon (HC) emissions[1], [2], [3].

2.2 Stratified charge

The stratified charge mode has the injection of fuel at high pressure during compression stroke and enables operation without a throttle which enables a globally leaner mixture to be used compared to homogenous mode [2]. The fuel is injected directly into the cylinder either close to or guided towards the spark plug. The mixture composition near the spark plug is compatible with stable ignition and flame propagation, whereas the mixture further away is much leaner. The use of stratified charge improves the BSFC significantly by reducing: pumping losses, heat losses, and chemical dissociation from lower cycle temperatures and it increases specific heat ratio [2]. Figure 2 below shows fuel consumption and specific NO_x emissions for the different operating modes [2]. It can clearly be stated that stratified charge is only an advantage for low load operation below 4bar BMEP, were a reduction in fuel consumption can be achieved. If stratified charge is extended towards higher loads, soot is likely formed due to regions of excessive fuel near the spark plug. The timing of the injection has also showed to be important. Early injection results in soot formation and to late injection can result in lean mixture and unburned HC emissions[1], [2].

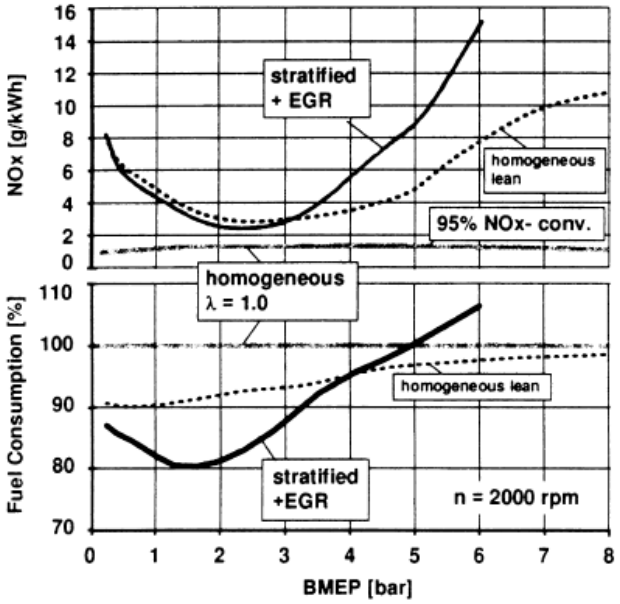

Figure 2. Fuel consumption and specific NO_x as a function of BMEP for homogeneous and stratified charged for a SIDI engine [2].

2.3 Lean operation

From Figure 2 it could be noticed that homogeneous lean operation offers a reduction in fuel consumption at lower loads compared to homogeneous stoichiometric. However it shows that stratified charge can reduce fuel consumption even more. With lean operation the ratio of specific heat increases with excessive air and thereby the thermal efficiency increases. The thermal efficiency of an ideal engine can be described by Equation (1), were specific heat ratio is denoted (C_p/C_v) and compression ratio r_c [2].

$$\eta = 1 - \frac{1}{r_c^{C_p/C_v - 1}} \quad (1)$$

Theoretically the thermal efficiency increases since specific heat ratio increases with leaner mixtures. Simultaneously the burn rate of the mixture decreases and at some point the mixture is to lean which results in incomplete combustions. This point is called the lean limit and usually a small window of misfiring with cycle to cycle variation of indicated mean effective pressure (IMEP) occurs as a result. Since combustion duration increases with leaner mixtures the power output decreases and so also the thermal efficiency. In order to gain benefits of lean burn engines the design of the combustion chamber needs to ensure a high burn rate in order to avoid counteract effects. To increase thermal efficiency and reduce emissions even more the lean limit could be extended. This is a complex problem since lean mixtures are hard to ignite and has a slow burn rate. Techniques which provide a stronger initial kernel or increase burn rate will be beneficial. One of the most important parameters determining burn rate is the turbulence level of the charge mixtures. The stratified charge mode has showed to extend the lean limit even more compared to homogenous mode, which enables a reduction in fuel consumption[1], [2].

3 Emissions from SI gasoline engines

The SI gasoline engine is a source of air pollution. The emissions from a SI engine can mainly be sorted into three groups of emissions: carbon monoxide (CO), HC and NO_x which is mostly nitrogen monoxide (NO) and a small amount of nitrogen dioxide (NO_2) [4]. NO and CO has direct effect on human health, whereas NO and HC contributes, in addition, to the formation of ozone and smog in the troposphere. These could result in deleterious effects on human health and visibility. PM emissions could be negligible for SI engines since it produces only small amounts, but is of great significance for CIDI engines. However concerns about small sized particles affecting human health has been increasing and may lead to regulations in future SI engines as well [5].

3.1 Emissions formation overview

Emissions are formed during the different phases in the four stroke operating cycle. NO and CO are formed through oxidation of N_2 and fuel in the bulk gases, whereas unburned HC arise from colder regions where the flame does not propagate [5]. The high flame temperature decomposes molecular oxygen (O_2) and N_2 from the air and composes it into NO and the main variable affecting NO formation is the high temperatures [4], [5]. CO is formed during the combustion process when there is insufficient oxygen (O_2) to oxidize all CO to CO_2, typically at richer mixtures. High temperatures can also be a source of CO formation due to dissociations of CO_2 [4]. Unburned HC emissions have several origins: crevices in the combustion chamber, oil film and incomplete combustion.

The effect of mixture composition on emission formation can be seen in Figure 3. The AFR has showed to be the most important parameter affecting the engine out emissions. Normally gasoline SI engines operate at stoichiometric conditions ($\lambda = 1$) to ensure that the TWC operation is satisfactory. Leaner mixtures results in lower emissions until combustion quality is jeopardized or even misfire occurs, which can be noticed when unburned HC rises rapidly. The stoichiometric AFR for gasoline is 14.7:1.

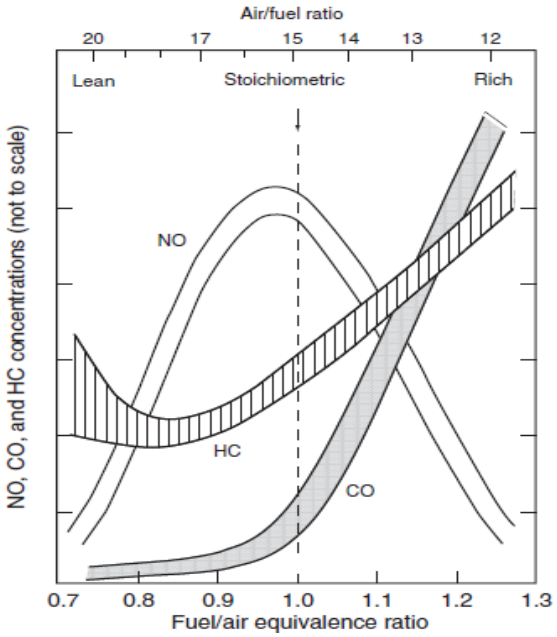

Figure 3. Emissions from SI gasoline engines at different AFR [4].

3.2 Formation of NO

NO forms principally when atmospheric nitrogen molecules oxidizes. Another possible source of NO is if the fuel contains N_2, and thereby oxidizes. This is usually the case of diesel fuels but could be negligible for gasoline fuels. NO is formed in the flame front and in the postflame gases. However in the combustion chamber the flame reaction zone is very small which results in a short residence time for NO formation. The majority of NO is therefore formed in the postflame burned gases. The exhaust gas temperature is dependent on when the mixture is burned, an early burned mixture reaches a higher temperature compared to a mixture burned late. The formation is strongly dependent on temperature and oxygen content, therefore mixture composition and ignition timing has a major influence on NO formation [4]. An early timing with fast burn rate will produce most NO due to high pressure and temperature. NO forms rapidly at high peak temperatures but formation freezes when temperature is below 1400K for stoichiometric conditions. NO formation is therefore somewhat higher at slightly leaner mixtures due to excessive O_2 and high temperatures, however as the mixture becomes even leaner the temperature decreases and so is also NO formation [5].

The mechanism of NO formation, close to stoichiometric conditions from atmospheric nitrogen is described by thermal route or the Zeldovich mechanism; see Equation (2), (3) and (4). The formation rate is slow compared to the overall combustion rate, though the rate increases exponentially with burned gas temperature [4].

$$O + N_2 \leftrightarrow NO + N \tag{2}$$

$$N + O_2 \leftrightarrow NO + O \tag{3}$$

$$N + OH \leftrightarrow NO + H \tag{4}$$

Another mechanism is the so called prompt mechanism of NO, which is active at the flame front. Approximation at stoichiometric conditions has showed that prompt mechanism has a contribution of 5-10% of the total NO formation. With diluted or lean mixtures this mechanism becomes more important when thermal NO is lowered [5].

3.3 Formation of CO

CO is formed due to incomplete formation into CO_2, which is a result of insufficient O_2. Due to the lack of O_2 the rich mixtures and fast expansion of the burned gases freezes the final oxidation process. In modern engines CO emissions is usually only a problem during cold starts and accelerations when the mixture is enriched [5]. The levels of CO observed in exhaust gases are lower than the maximum levels in the combustion chambers, but significantly higher than equilibrium values for exhaust conditions. The process which governs CO concentration is kinetically controlled, see Equation (5).

$$CO + OH \leftrightarrow CO_2 + H \tag{5}$$

The reaction takes places in both directions. At long residence time equilibrium occurs between the reactions and this equilibrium is mainly temperature dependent. At higher temperature dissociations increases and the reaction strikes towards to the left side and CO increases. Even though the temperature is low, a small amount of CO concentration is present due to slow formation of OH [6].

3.4 Formation of HC

HC emissions are a result of incomplete combustion of hydrocarbon fuels. Unburned HC emissions are a result of the mixture being in contact with cold layers or surfaces, for example the cylinder wall which prevents oxidation during flame passage. The unburned HC can later be oxidized in the burned gas during expansion stroke. A fraction is left in the cylinder and the remaining HC leaves the cylinder into the exhaust system as engine out HC. There exists a variety of different HC compounds in exhaust gases and it can be divided into non reactive and reactive compounds based on their potential for oxidant formation in photochemical smog. Fuel composition with higher proportions of aromatics and olefins produces higher concentration of reactive HC [4], [5].

The major contributor to HC emissions during steady state operation can be addressed to the crevices in the piston ring land and narrow passages in the combustion chamber. During compression stroke, these volumes are filled with mixture. During expansion the gas leaves the crevices when pressure decreases and a part of the unburned HC is oxidized in the burned gas. The final product of HC emissions depends on volume, location of spark plug and operating conditions. Crevices will contribute to HC emissions if the flame does not propagate through its volume and if the unburned HC fail to oxidize later in the burned gas [5].

The oil film absorbs fuel vapor on the cylinder walls during intake and compression stroke. Desorption of the fuel vapor occurs during the expansion and exhaust stroke which results in possible unburned HC. The last primary formation mechanism is incomplete combustion as a result of misfiring or low combustion efficiency. This could happen due to incorrect mixture composition for example due to EGR or bad injection or ignition timing.

3.5 Emissions of lean burn engines

From an engine out emissions perspective the lean burn engine is a good strategy for low fuel consumption and low emissions. Even though NO_x formation is lowered, TWC reduction of NO_x is not possible, however CO and HC oxidation is still possible at lean operation. This means that NO_x emissions are the major problem in gasoline lean burn SIDI engines. Different exhaust aftertreatment systems can then be used to reduce the remaining NO_x, however these techniques has some drawbacks and tradeoffs with high costs, sulfur poisoning and advanced control strategies.

4 Catalytic converters

For some decades, the catalytic converters based on PGMs have been the primary technology to reduce polluting emissions. The demands on improved catalytic converters and new alternative technologies are increasing as newer stricter legislations of emission limits are proposed. In this chapter the most common types of catalytic converters are explained and described.

4.1 Introduction to catalytic converters

Catalytic converters generally have a monolithic honeycomb substrate support. The substrate support can consist of different material compositions but is often ceramic or metallic. It is built up to increase the effective surface with active sites which interacts with the bypassing exhaust gas. There exist different designs of the substrate, each with their respective advantage and disadvantage. Examples of different substrate designs can be seen in Figure 4 below. For example, a honeycomb substrate has a large surface area but meanwhile it induces a pressure drop over the catalyst with increased exhaust backpressure as a result.

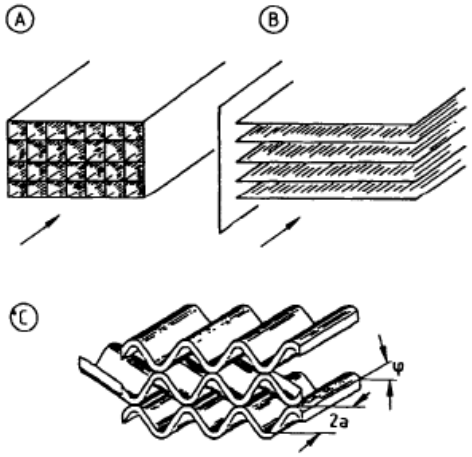

Figure 4. Different monolithic substrate designs, a) honeycomb, b) laminar with straight layers, c) laminar with wavy layers [8].

A thin layer containing a mixture between PGM and other oxides is applied on the support to increase the intensity of catalyst reactions, this is called the washcoat. When the washcoat is applied it forms an irregular surface on the supporting substrate which increases the active site surface even more.

The composition of a washcoat depends on the required properties such as activity, selectivity, stability and accessibility. When evaluating these parameters there is always a tradeoff to consider. Activity is promoted by higher temperatures but meanwhile the thermal stability is demoted. High selectivity is desirable as it produces high yields of a desired product and suppresses unwanted and consecutive reactions. A good stability is desired to prevent loss of selectivity, activity or mechanical strength of the catalytic converter. It is only in theory a catalytic converter is found unchanged after a reaction has occurred. All catalysts age and when the activity or selectivity become insufficient they require regeneration to restore their catalytic properties. [7].

Deactivation of activity on a catalytic converter can occur due to many factors. Deactivation can either be reversible or non reversible, depending on the type of

deactivation that occurs. For instance, a catalytic converter exposed to excessive temperature in the exhaust gas will be deactivated through sintering of the active sites. This causes permanent damages on the catalytic bed and cannot be regenerated. Deactivation through poisoning can also occur due to impurities in the fuel such as SO_2. Impurities stick to the active sites and blocks the desired reactions to occur. This process is reversible and regeneration can be achieved by burning off the impurities at high exhaust temperature.

The catalyst substrate is made of a ceramic or metallic material with an active coating called a washcoat. The washcoat mainly contains a combination of the precious metals: platinum (Pt), palladium (Pd) and rhodium (Rh). The composition can also include other materials such as cerium, alumina and other oxides. The applied washcoat on the catalysts substrate can consist of many different compositions depending on what type of reactions that are desired. Pt and Pd have showed excellent properties to accelerate the oxidation of HC and CO meanwhile Rh is better to accelerate the reduction of NO_x. The more commonly used compositions are a base with Pt-Rh or Pd-Rh, where one material accelerates the reduction and the other one accelerates the oxidation [9].

4.2 Three Way Catalyst

The most common type of catalytic converter in a passenger vehicle is a TWC. A TWC operates in a so called closed loop system. This includes an oxygen sensor called lambda sensor (λ) to be able to control the AFR [10].

The TWC has three tasks, reduce NO_x into N_2 and O_2, oxidize CO to CO_2 and to oxidize unburned HC to CO_2 and water (H_2O). The following reactions take place in a TWC at stoichiometric conditions ($\lambda = 1$).

Reactions with O_2 (oxidation) [11].

$$C_mH_n + (m + 0.25n)O_2 \rightleftharpoons mCO_2 + 0.5nH_2O \quad (6)$$

$$CO + 0.5O_2 \rightleftharpoons CO_2 \quad (7)$$

$$H_2 + 0.5O_2 \rightleftharpoons H_2O \quad (8)$$

Reactions with NO (oxidation/reduction) [11].

$$C_mH_n + 2(m + 0.25n)NO \rightleftharpoons 1(m + 0.25n)N_2 + mCO_2 + 0.5nH_2O \quad (9)$$

$$CO + NO \rightleftharpoons 0.5N_2 + CO_2 \quad (10)$$

$$H_2 + NO \rightleftharpoons 0.5N_2 + H_2O \quad (11)$$

At rich conditions ($\lambda < 1$) additional reactions takes place [11].

$$CO + H_2O \rightleftharpoons CO_2 + H_2 \quad (12)$$

$$C_mH_n + 2mH_2O \rightleftharpoons mCO_2 + (2m + 0.5n)H_2 \quad (13)$$

A TWC is as most efficient when the exhaust gas composition from the engine is cycling around stoichiometric conditions. This occurs when the AFR is between 14.6 and 14.8 for gasoline. Within this window the conversion of all three polluting emissions is almost complete, although outside this window the efficiency decreases rapidly [10].

When the engine operates lean, oxidation of CO and HC is favored at the expense of NO_x. When the opposite condition occurs, the reduction of NO_x is favored at the expense of CO and HC [4], [11].

4.3 Lean NO_x Trap

A Lean NO_x Trap (LNT) is mainly used in vehicles with a SIDI engine for taking care of the NO_x emissions during lean operation. Comparing the basic structure between a LNT and a TWC shows they are almost the same, but in a chemical point of view they are somewhat different.

A LNT is also known as a NO_x absorbing catalytic converter. The catalytic washcoat generally consists of a PGM composition with an additional NO_x absorbing agent. A LNT operates in two modes, either in sorption (oxidation) or regeneration (reduction). In sorption mode when the engine operates lean, the engine out NO_x is absorbed and stored in the trap. In regeneration mode, when the engine switches from lean to rich mode, the rich mixture reaches the LNT and reacts with the stored NO_x and the final products are N_2 and H_2O. The washcoat of a LNT often contains barium oxide (BaO) which has proven to be a good NO_x absorbing material [12]. A conceptual layout of a LNT aftertreatment system can be seen in Figure 5.

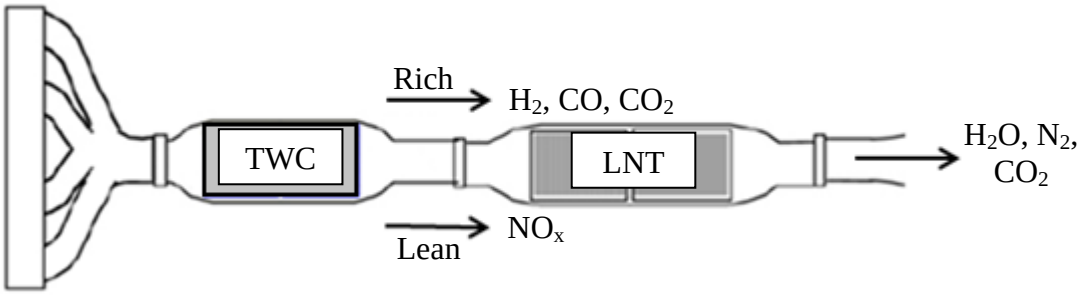

Figure 5. Conceptual layout of a LNT aftertreatment system.

The NO_x storage capacity depends on the active surface sites of the washcoat and is often very limited. The storage capacity are often filled within 30 – 120s during lean operation and regenerated within 1-10 seconds. [12].

The basic structure of TWC and LNT catalytic converters are equivalent. The basic substrate is a monolith with a design that increases the surface of active PGM sites. The main difference between these catalytic converters is the washcoat composition which differs as the LNT has a NO_x absorbing agent included. Another difference is the operating temperature range for a conventional LNT which is between 200 – 500 °C. A TWC has typically an operating range from 150 °C and can sustain temperatures up to 900°C without causing any permanent damage. During stoichiometric conditions both the TWC and LNT operates in the same way and the same type of chemical reactions occurs. But when the engine operates lean neither of the catalytic converters can reduce NO_x emissions. However the LNT stores the NO_x on the catalyst bed until the engine operates rich and the stored NO_x can be reduced [13].

4.4 Selective Catalytic Reduction

The SCR catalyst was at the beginning introduced on stationary power plants and stationary engines, but is nowadays a common aftertreatment system for heavy duty diesel engines. By using a SCR catalyst it is possible to reduce NO_x emissions and at

the same time reduce fuel consumption. It enables the diesel engine to operate in areas where lower fuel consumption is achieved and lower PM is formed but where engine out NO_x emissions are increased.

The purpose of a SCR catalyst is to convert NO_x with the aid of a reductant agent into N_2 and H_2O. Mostly a gaseous reductant is used, generally urea, anhydrous or aqueous NH_3. Pure anhydrous NH_3 is extremely toxic and difficult to handle in a safe way and requires no further conversion. Aqueous NH_3 requires to be hydrolyzed in order to function but meanwhile is significantly safer to store. Urea is the safest to store but requires first conversion to NH_3 through thermal decomposition to function as an efficient reductant. The reductant is generally injected from a separate dosing system into the exhaust gas stream where it is absorbed on the catalyst further down the exhaust system. With the use of NH_3 and the presence of excess oxygen the SCR catalyst can reduce up to 70 – 95% of the engine out NO_x [16]. A conceptual layout of a SCR aftertreatment system can be seen in Figure 6.

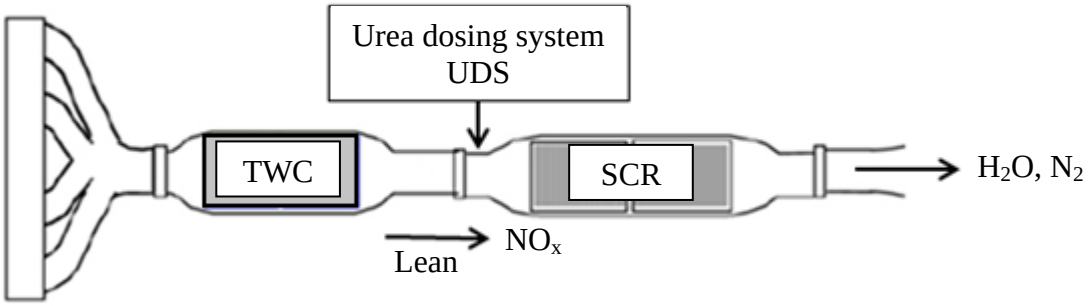

Figure 6. Conceptual layout of a SCR aftertreatment system.

A SCR catalyst requires to be located at a certain distance from the exhaust port as it is relative temperature sensitive compared to an ordinary TWC. The ideal reaction takes place between temperatures of 350 – 450 °C, however it can operate down to 200 °C but with decreased NO_x reduction efficiency as a consequence.

The SCR substrate is often manufactured from ceramic materials such as titanium oxide, vanadium, tungsten, zeolites or similar precious metals. All catalysts have their respective advantage and disadvantages. Thermal stability is especially important for automotive SCR applications. The use of zeolite catalyst allows operation at significantly higher temperatures compared to base metal catalysts. It has the ability to withstand long term operation at 650 °C and transient conditions of up to 800 °C for short amount of time. Zeolite catalysts are also not as sensitive to SO_2 poisoning upon the active sites of the catalyst [16], [17].

At the catalyst bed the following reactions takes place with anhydrous NH_3 [16].

$$4NO + 4NH_3 + O_2 = 4N_2 + 6H_2O \quad (14)$$

$$6NO_2 + 8NH_3 = 7N_2 + 12H_2O \quad (15)$$

If urea is used instead an additional preceding reaction takes place [16].

$$4NO + 2(NH_2)_2CO + O_2 \rightarrow 4N_2 + 4H_2O + 2CO_2 \quad (16)$$

5 Passive SCR

The passive SCR aftertreatment system concept for lean burn gasoline engines includes a TWC and one or several SCR catalysts. NH_3 is formed during rich operating periods over the TWC and is stored in the SCR catalyst further down the exhaust system. During the following lean cycle, engine out NO_x emission reacts with the stored NH_3 and forms N_2 and H_2O. A study has showed NO_x reduction efficiency up to 90% is possible [22]. Since the fuel penalty is of great importance, the NH_3 formation during the rich cycle should be maximized with as minimal fuel penalty as possible. Since rich operation disenables oxidation of HC and CO over the TWC the problem is to create NH_3 without increasing CO and HC emissions. Equation (17) describes the reaction kinetics during rich condition and Equation (18) describes it under lean conditions. A conceptual layout of the passive SCR aftertreatment system can be seen in Figure 7.

$$NO_x + H_2/CO \leftrightarrow NH_3 + CO_2 + H_20 \quad (17)$$

$$NO_x + NH_3 \leftrightarrow N_2 + H_2O \quad (18)$$

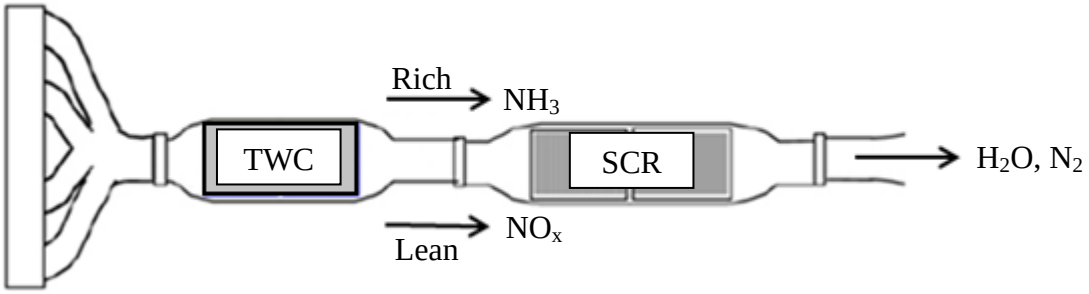

Figure 7. Conceptual layout of a passive SCR aftertreatment system.

The NH_3 storage capacity depends on the composition and bed temperature of the SCR catalyst [22]. Two types of zeolite based catalysts are commonly used in SCR catalyst, copper (Cu) and iron (Fe) zeolites. As the temperature increases the NH_3 storage capacity decreases until it reaches 400 °C. Beyond this temperature it could be assumed to be negligible, which is a problem for high load operation. This applies for both catalysts but Cu-based has better storage capacity as the temperature decreases [22]. In order to reduce tailpipe NO_x emissions on high loads, typical highway driving, one or more SCR catalysts are placed further down the exhaust system to achieve a lower bed temperature and thereby cover a larger operating range.

A possible problem with this system is NH_3 slip may occur if the formed NH_3 is passing through the SCR catalysts. It is therefore important to ensure SCR catalyst storage capacity is enough and no slip occurs.

6 Ammonia formation factors

The NH_3 formation over a TWC is affected by many factors, the literature in this field is limited and only a handful of studies have been carried out. The following chapter describes some of the most important factors affecting the NH_3 formation.

6.1 Sulfur level

There is a variety of different compounds which can deactivate a catalyst, the most recognized involves sulfur absorption on metals. When SO_2 is absorbed on active sites, a new chemical compound is formed which has a different catalytic activity. The activity is generally heavily reduced, but it would not necessarily mean that the site becomes totally inactive [18].

Studies showed that the sulfur level in fuels is of great importance to how much NH_3 that is formed over the TWC during rich conditions. The highest concentrations of possible formed NH_3 is when there is absence of sulfur. If the amount of sulfur is increased it will promote the formation of N_2O and inhibit the formation of NH_3. This can be seen in Figure 8 below [19]. A study has showed that the amount of NH_3 is greatly reduced as soon as sulfur is introduced into the fuel [20].

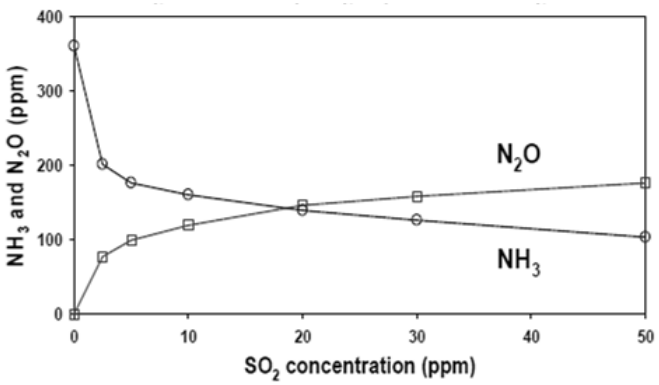

Figure 8. Effect of low sulfur gasoline upon NH_3 and N_2O [19].

6.2 Composition of a TWC

In Figure 9, different TWC compositions have been experimentally tested to evaluate how the NH_3 formation is affected during a rich pulse. Cerium (Ce) increases the amount of O_2 that can be stored in the TWC and thereby increasing the oxygen storage capacity (OSC). Ce in combination with Pd, Pd-Rh or Pt-Rh seems to have great positive effects on the NH_3 formation among the tested TWCs. NH_3 is represented by the dotted line in Figure 9 [14].

Another study has showed that a Pd-Rh with OSC compared to Pd-only TWC has a negative effect on the NH_3 formation during transient conditions [15]. The result showed that the cumulative amount of NH_3 is higher for a TWC with Pd only during the NEDC cycle. In this study it is not mentioned if Ce is the primary OSC material. However these two studies contradict each other regard to the impact of OSC for the NH_3 formation.

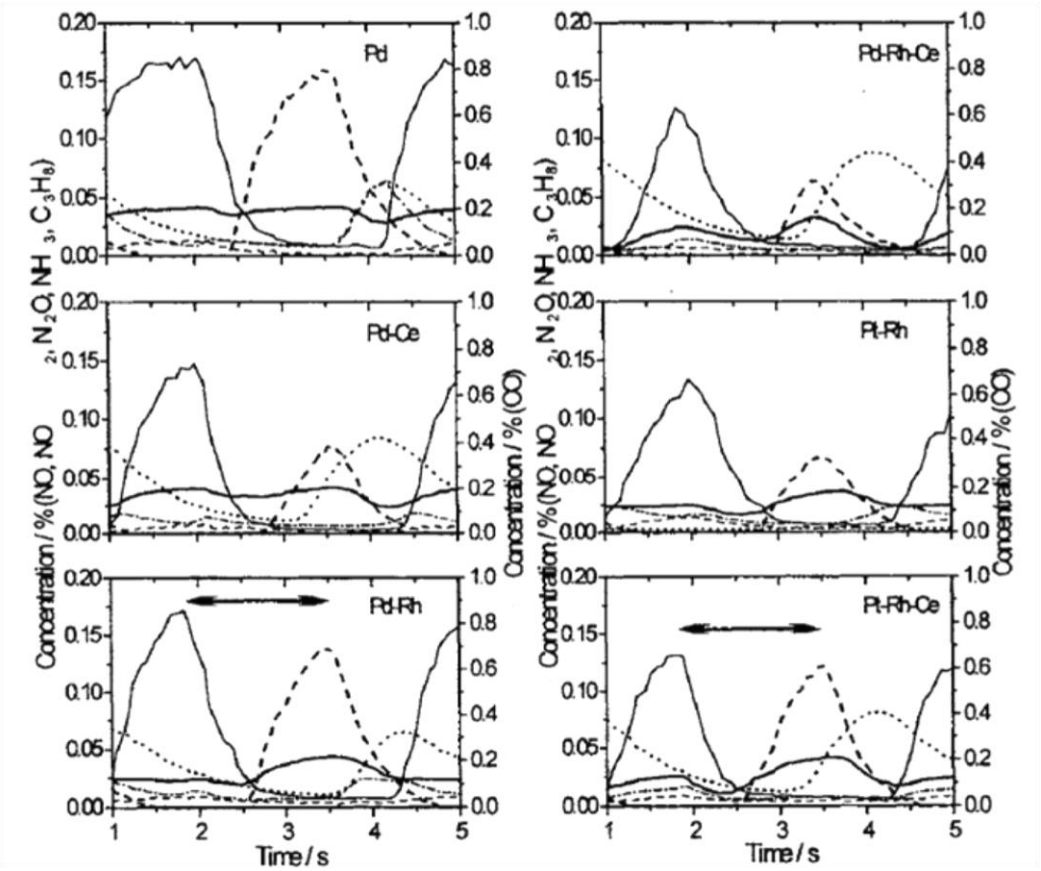

Figure 9. NH_3 formation (dotted line) due to TWC compositions [14].

How the PGMs Rh, Pt and Pd are composed in a TWC affects the NH_3 formation. From Figure 10 below a comparison between a Pd only and a Pd/Pt/Rh TWC is made. It clearly shows that the formed NH_3 concentration is higher for Pd/Pt/Rh for slightly richer mixtures but they approach the same level of NH_3 formation as the mixture is enriched [20]. This indicates it is possible to compose a customized catalytic composition for a TWC to meet the demands to form as much NH_3 as possible for as less rich mixture as possible.

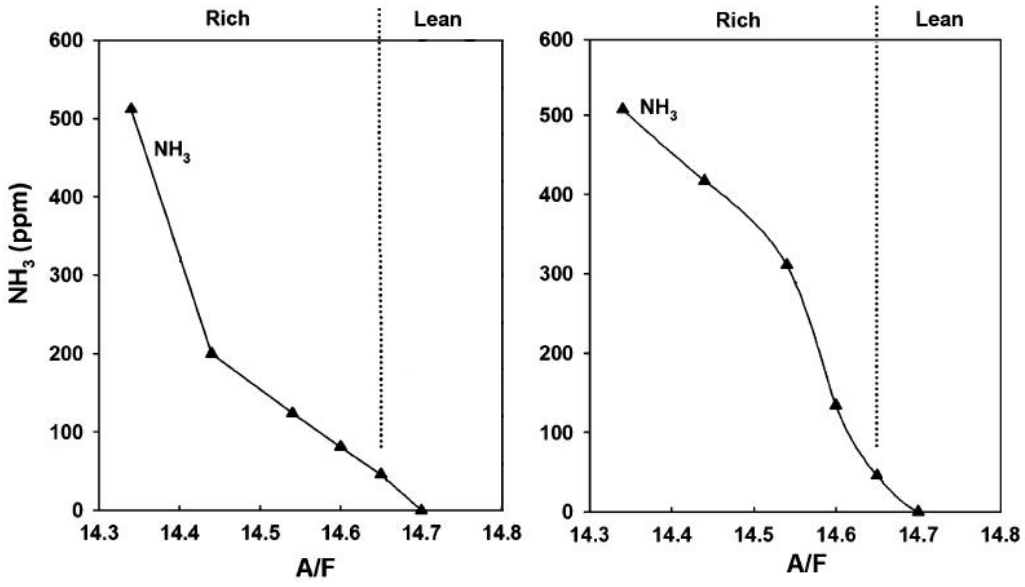

Figure 10. NH_3 formation of Pd only (left) and Pd/Pt/Rh TWC (right) [20].

6.3 Rich cycle duration

The NH_3 formation in relation to rich cycle duration in an LNT has been studied earlier [21]. The behavior of NH_3 formation is presumed to be similar for a TWC. The results from the LNT studies will therefore be used as guidelines.

The formed NH_3 should be proportional to the accumulated duration of the rich cycles, which means it should be independent of cycling frequency during ideal conditions. However in practice the mixture is not instantly as rich or lean as it is intended to be. Increased cycling frequency makes the mixture less homogeneous compared to a lower cycling frequency. A lower cycling frequency is therefore preferable to promote the largest concentrations of NH_3 [21]. Figure 11 shows that the concentration of NH_3 increases with increased cycle duration [21]. The ratio between rich/lean cycle time is 1:9 which results in a rich cycle of 1/10 of the total cycle duration. From the study it could therefore be stated that increased rich cycle duration increases the concentration of NH_3.

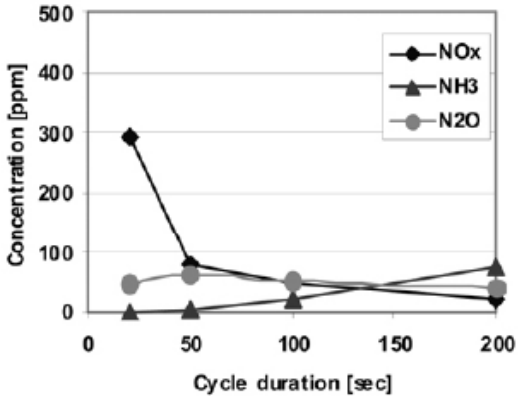

Figure 11. NO_x, NH_3 and N_2O formation as a function of cycle duration for a LNT [21].

6.4 Air-to-fuel ratio

Studies have shown the impact of AFR on NH_3 formation [22], [23]. Maximum NH_3 formation was obtained between AFR 14.0-14.2 during an AFR sweep, see Figure 12. The sweep was carried out at 2000rpm, 2bar BMEP with a catalyst bed temperature between 550 - 600 °C. NO_x, CO and hydrogen (H_2) are required in order to form NH_3 according to theory. At less rich conditions engine out H_2 decreases and limits the formation of NH_3. During richer conditions the NH_3 formation is limited by the decreased amount of engine out NO_x. In order to form maximum NH_3, AFR should be held at 14.2:1 according to these results. The fuel used during the experiment was standard reformulated gasoline with 30 ppm sulfur.

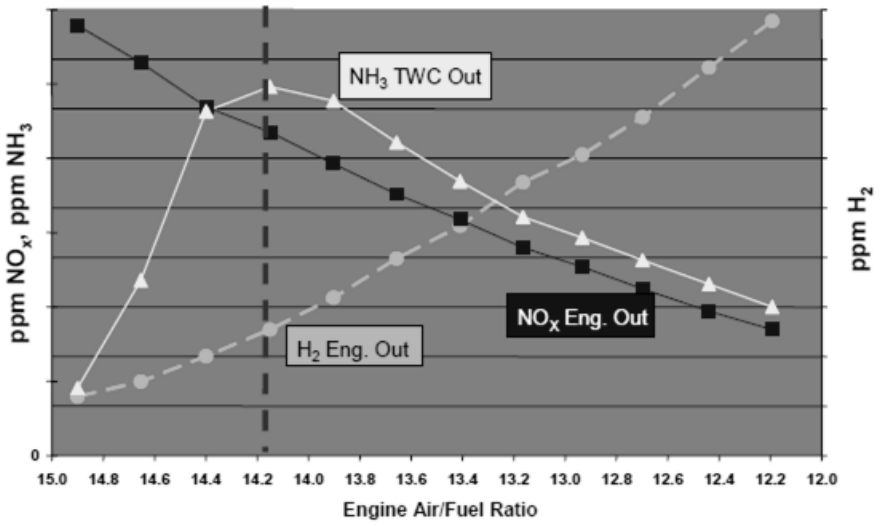

Figure 12. AFR sweep test for NH_3 formation on a TWC [22].

The catalyst bed temperature has showed to influence NH_3 formation [24]. Measurements during cold starts showed NH_3 is first present when catalyst light-off has occurred [24]. Experiments were conducted on four Euro-3 passenger vehicles on chassis dynamometer. During acceleration the measurements showed an increased level of NH_3 and H_2 and during deceleration a decreased level of NH_3. This could be explained by the rich mixtures during acceleration even though the exhaust gas temperature likely increased at higher loads.

7 Experiments

The experiments were carried out in an engine test cell at Chalmers University of Technology. A description of the experimental setup regarding hardware, software and test plan are described below.

7.1 Engine and related systems

The experimental tests in this master thesis were carried out on a modified Volvo SI6 engine. It is a SIDI naturally aspirated 3.2 liter inline 6 cylinder engine with four valves per cylinder. This engine can be found in newer Volvo V70, S80 and XC90.

Table 1. Technical specification of the experimentally tested engine.

Engine	**B6324S**
Type	In-line, 6-cylinder naturally aspirated
Injection	Direct injected
Ignition	Spark ignited
Displacement (cm^3)	3192
Bore/Stroke (mm)	84 / 96
Combustion chamber type	Pent-roof
Compression ratio	11.4:1
Valves, no/cylinder	4
Max output, kW (hp) / rpm	175 (238) / 6200
Max torque, Nm/rpm	320 / 3200

The exhaust system was customized to meet the demands of the experiments. As the engine is equipped with closed coupled catalysts (CCC) which are TWCs mounted near the exhaust ports (1), the analysis will only be carried out at one of the catalysts (cylinder 4-6). The standard exhaust system from Volvo Car Corporation (VCC) contained additional TWCs which are called under floor catalysts (UFC). These TWCs were removed and replaced with regular exhaust pipes. On the studied bank an exhaust gas cooler (3) was installed after the flexible pipe (2). This was done to be able to cool the exhaust gases before they enter the SCR catalyst (4). The SCR catalyst was installed after the cooler and after the SCR catalyst both pipes merged into one pipe (5). In Figure 13 an overview of the exhaust system can be seen and descriptions are found in Table 2.

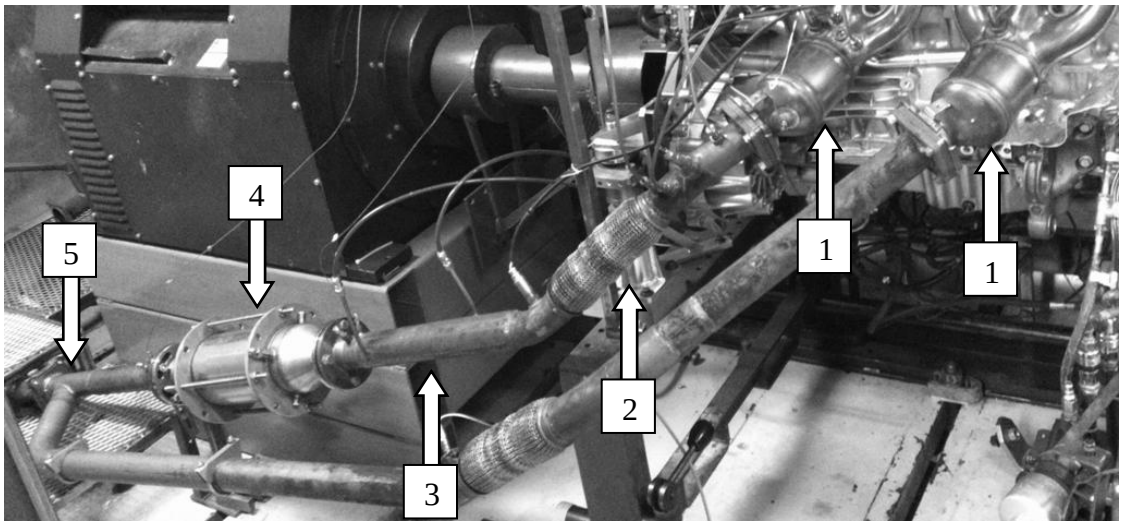

Figure 13. Overview of the modified exhaust system.

Table 2. Description of the modified exhaust system.

Point	Description
1	Closed coupled catalysts (CCC)
2	Flexible pipe
3	Exhaust gas cooler
4	SCR catalyst
5	Merging pipes

7.1.1 Three way catalysts

In this project two types of TWCs were experimentally tested and provided from VCC. The substrates have the same total volume and cross sectional area but have different geometry and charge of PGM in the washcoat. The geometry of the two different TWCs can be seen in Figure 14 below. The properties are represented in Table 3.

Table 3. Properties of the TWCs.

Property	TWC 1	TWC 2
Geometry	Elliptic cylinder	Circular cylinder
Number of cells	400	600
Cross sectional area (cm^2)	80	80
Total Volume (cm^3)	800 (approximately)	800 (approximately)
Composition, Pt:Pd:Rh (g/ft^3)	10:60:10	0:45:2
Total charge (g/ft^3)	80	47

Figure 14. Elliptic TWC 1 to the left and circular TWC 1 to the right.

7.1.2 Selective catalytic reduction catalysts

There is little information available for the SCR catalysts tested in this master thesis. Both VCC and HT provided one SCR catalyst each to this project. They are both copper-zeolite based and have most certainly different additives. The catalyst substrate from VCC is smaller in volume and diameter than the SCR catalyst provided

from HT. Both SCR catalysts can be seen in Figure 15 below and the properties are represented in Table 4.

Table 4. Properties of the SCRs.

	SCR 1	**SCR 2**
Brand	VCC	Haldor Topsøe A/S
Substrate	Copper-Zeolite	Copper-Zeolite
Dimensions (ØxL, cm)	12,5x15,2	14,4x7,6
Cross sectional area (cm^2)	122	162
Total Volume (cm^3)	1900 (approximately)	2500 (approximately)
No. of substrates	1	2

Figure 15. VCC SCR to the left and Haldor Topsøe A/S SCR to the right.

7.2 Experimental test setup

The used hardware and corresponding software for the experiments are explained and described below.

7.2.1 Hardware

The exhaust system was equipped with additional sockets to connect sensors and probes to measure desired parameters. These additional sockets were wideband lambda, temperature, pressure and emission probe sockets. The locations of the sockets can be seen in Figure 16 and the descriptions are represented in Table 5.

Table 5. Description of added sockets to the TWC and first part of the exhaust system.

Point	**Description**	**Point**	**Description**
1	Pressure pre TWC	6	Pressure post TWC
2	Temperature pre TWC	7	Lambda post TWC
3	Emissions pre TWC	8	NH_3 post TWC
4	Lambda pre TWC	9	Emissions post TWC
5	Temperature post TWC		

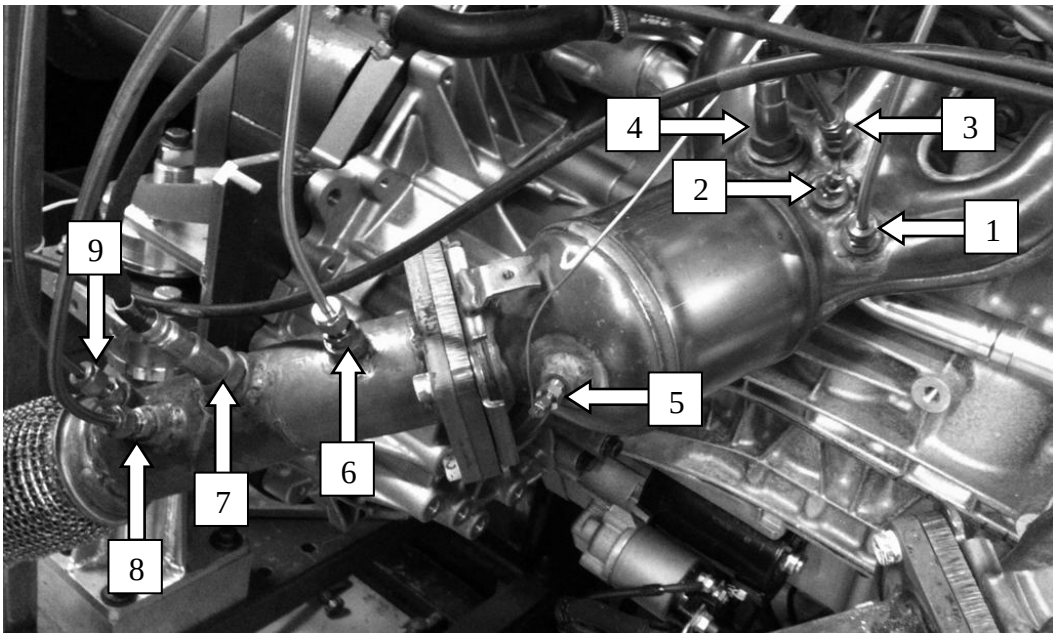

Figure 16. Location of added sockets to the TWC and first part of the exhaust system.

All three wideband lambda sensors were monitored with ETAS Lambda Meter LA4 modules. One lambda sensor was connected pre and one post the TWC on the studied (left) bank and one pre the TWC on the right bank. The wideband lambda on the right bank was installed to ensure that the engine operated equally over all cylinders.

The engine was equipped with a Kistler pressure gauge type 6053CC60U20 on the first cylinder to monitor the in-cylinder pressure. This is a fast pressure gauge with a high sampling rate. It is mounted directly in the cylinder head by drilling a small hole into the combustion chamber. The in-cylinder pressure gauge was connected to a charge amplifier which in next turn was connected to an AVL IndiMaster. To determine the position of the crankshaft a high resolution crankshaft position sensor were connected to the front end of the crankshaft. Together with the in-cylinder pressure signal, signals for the injection, ignition and crankshaft position were connected to the AVL IndiMaster as well. The AVL IndiMaster performs realtime calculations which are sent to the related IndiCom software. With this software it is possible to monitor all desired parameters. In this case it was the in-cylinder pressure, injection, ignition timing and knock of the engine which were the most important parameters.

To manage and monitor the engine control unit (ECU), VAT2000 was used. This was required to be able to change lambda value, throttle position and ignition to control the load. To be able to communicate with the ECU an amplitude modulation (AM) module was used. This is a dedicated computer controlling the in- and outgoing communication between VAT2000 and the ECU. For example it is responsible of retrieving all measured states on the engine into VAT2000. There was also an analogue input module connected to the AM-module, this was to monitor for example engine oil pressure and analogue outputs of the wideband lambda sensors. The ETAS Lambda Meter LA4, charge amplifier, AM-module, analogue input module and AVL IndiMaster can be seen in Figure 17 below.

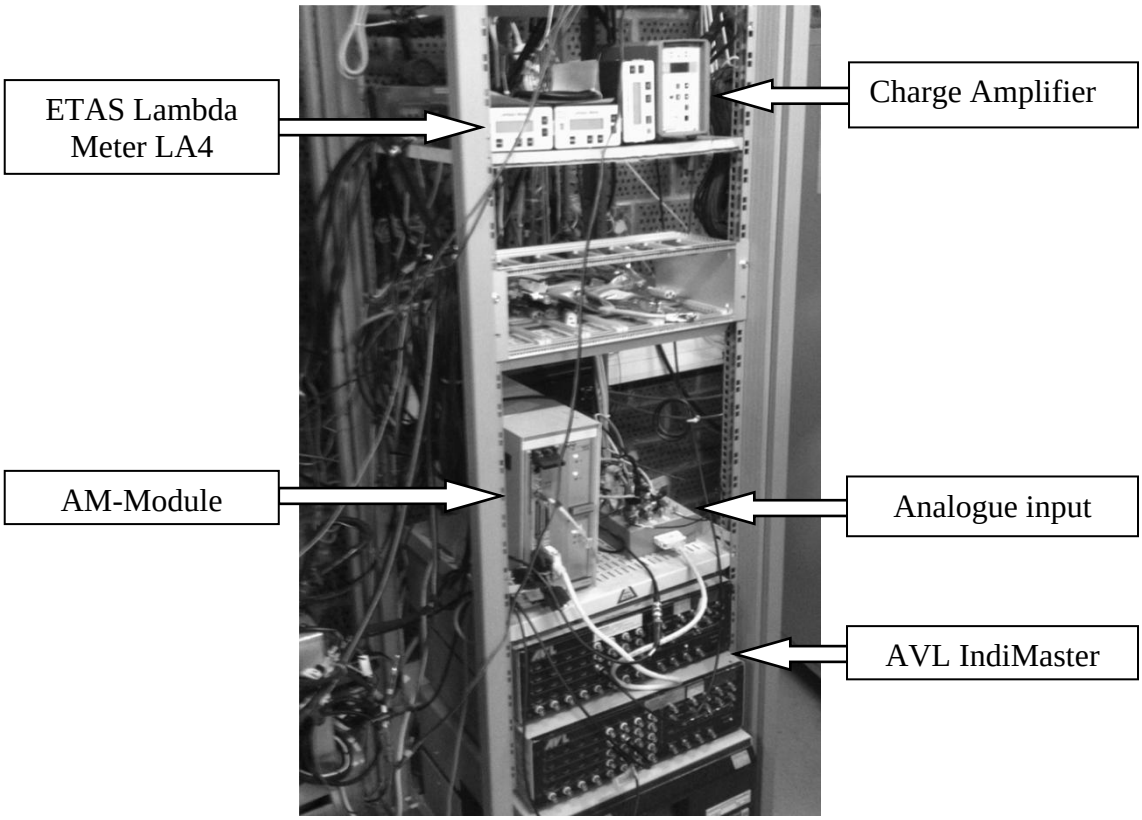

Figure 17. ETAS Lambda Meter LA4, charge amplifier, AM-Module, analogue input module and AVL IndiMaster.

To monitor temperatures, type K thermocouples were used. Wika type A-10 pressure gauges were attached to the exhaust system pre and post TWC to monitor the exhaust back pressure. The thermocouples and pressure gauges were connected to a National Instruments DAQ unit. Both pressure and temperature were retrieved from the DAQ units as signals into a LabVIEW program.

To measure the fuel flow a MicroMotion fuel mass flow sensor was used. This system is accurate and fast, it presents the real time value of the fuel flow on an external display and a signal was sent to the LabVIEW program. An additional system to measure the fuel flow was also used which was an AVL fuel balance. This system was only used to verify the result from the MicroMotion unit since it was already connected and ready to use.

Emission probes were attached pre and post the TWC for the initial tests. For the succeeding tests the probes were repositioned to measure pre and post the SCR catalyst. An emission sample was extracted to the emission equipment were the sample was analyzed. Separate emission signals was sent to a National Instruments DAQ unit which sent signals to the LabVIEW program. In Figure 18 below the emission analyzer equipment used can be seen. Unfortunately the HC measurement equipment was out of order during the experiments.

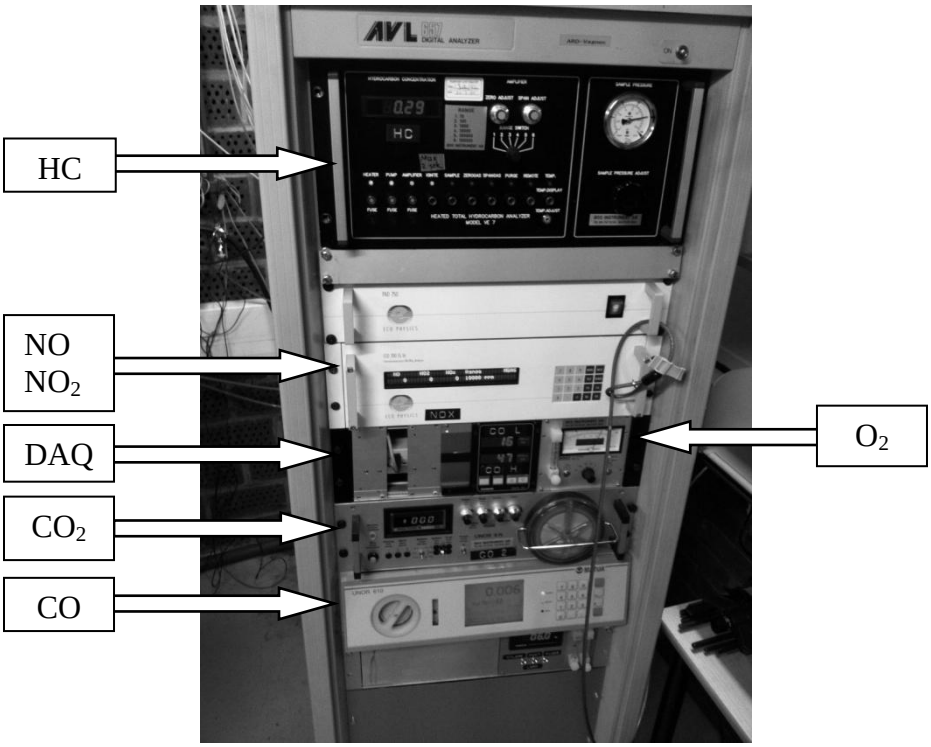

Figure 18. Emission analyzer equipment.

NH_3 was measured with a Gasmet CX-4000 fourier transform infrared (FTIR) instrument, which use a technique of infrared spectroscopy. A sample of the exhaust gases is extracted from the main stream and is exposed for infrared radiation. Depending on the composition of the molecules in the sample, the resulting spectrum transmitted by the gas will always be unique, as a molecular fingerprint. This makes a FTIR useful to identify unknown substances, determine the quality or consistency of a sample and determine the amount of components in a mixture [25]. The main advantage of a FTIR is that it has the ability to measure all substances simultaneously. This makes it useful if several components are of interest. Together with the FTIR the corresponding Calcmet software was used which is a stand-alone system. This software was used because no analogue signal was available from the FTIR equipment.

Additional sockets were attached to measure NH_3, one before and one after the SCR catalyst. Also, additional temperature sockets were added onto the SCR catalyst to measure the temperature of the bed and of the in- and outgoing exhaust gas. The added sockets for the SCR catalyst and FTIR can be seen in Figure 19. The description of the added sockets can be found in Table 6.

Table 6. Description of added sockets to the SCR catalyst and second part of the exhaust system.

Point	Description	Point	Description
1	Temperature pre SCR	4	Temperature post SCR
2	Temperature brick 1	5	NH_3 post SCR
3	Temperature brick 2	6	Emissions post SCR

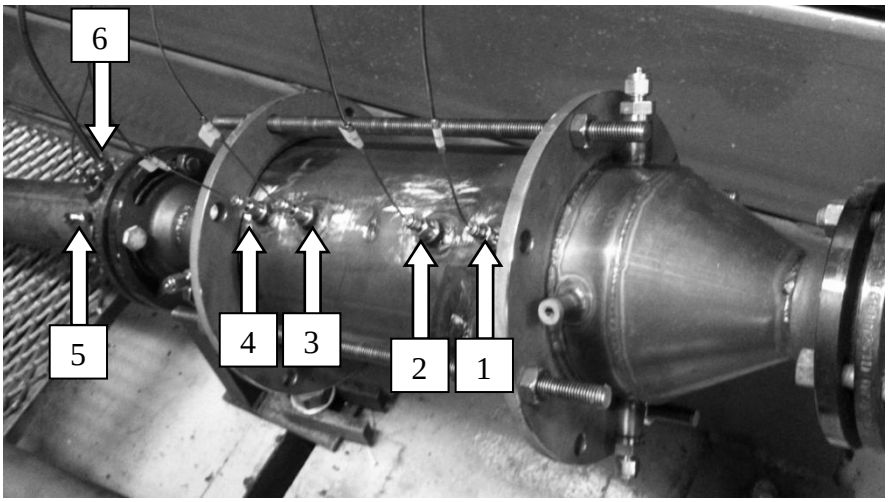

Figure 19. Overview of added sockets to the SCR and the second part of the exhaust system.

The engine was mechanically connected to an electrical dynamometer type AVL Elin through the rear end of the crankshaft. The dynamometer had an external control panel were it was possible to either regulate the engine with speed or torque. In this project the dynamometer was controlled by regulating the desired engine speed.

7.2.2 Software

In this master thesis different software has been used to ease the experiments and analysis of the results. In this section the software used will be given a brief explanation.

7.2.2.1 VAT2000

VAT2000 is an abbreviation for Volvo Application Tool. This is an application developed within Volvo for optimizing and managing PDF for control modules. PDF is an abbreviation for program and data file which contain all parameters for the engine to operate in a desirable state. This software is independent of supplier which means a PDF from any supplier can be used. VAT2000 uses the European ASAP standard, were except from Volvo also BMW, Mercedes, Bosch and Siemens are included.

This software was used to monitor and tune the engine parameters during the experimental tests. Throttle angle, lambda and ignition timing parameters were changed to achieve the target operating point.

7.2.2.2 LabVIEW

LabVIEW is an abbreviation for Laboratory Virtual Instrumentation Engineering Workbench. It is a tool to develop measurement, test and control systems in a graphical environment by using intuitive icons and wires to resemble a flowchart. This software was used to create an application to measure and log desired analogue data such as emissions, temperatures, pressures and lambda. The analogue signals were sampled with three DAQ units. The first DAQ measured emissions, the second pressures and the third temperatures. DAQ one and two sampled with a frequency of 1 kHz and a mean value of 1 Hz was logged. DAQ number three sampled temperatures from the thermocouples at 0.5Hz, which was the maximum sample rate. LabVIEW measured the signals continuously and a manual trigger for data log was used to save the results to a text file.

7.2.2.3 Calcmet

Calcmet was used to analyze the sample spectrum from the FTIR to determine the NH_3 concentration. During a measurement selected emissions levels were presented as current values and could also be presented as graphical trends. The results were saved to a text file containing emissions with corresponding time.

7.2.2.4 Matlab

Matlab is an application which performs intense computational tasks a lot faster than traditional programming languages. Matlab was used to analyze the saved result from LabVIEW and Calcmet. The sampled text files were imported into Matlab where analysis of the sampled data was carried out.

7.2.2.5 AVL IndiCom

AVL IndiCom is an application to monitor ongoing combustion processes. It was possible to build custom panels to suit the needs of experiments. The AVL Indicom software was used to monitor the in-cylinder pressure, ignition and injection timing and knock levels of the engine. The parameters were presented in real time as either numeric values or graphs.

7.3 Experiment plan

A description of the planned experiments is described in the following section.

7.3.1 Ammonia formation steady state

The objective with this experiment was to determine the NH_3 formation over the TWC with regard to engine speed, engine load, lambda and TWC composition. The NH_3 was measured continuously for a fixed operating point. The test matrix for this experiment is showed in Table 7.

Table 7. Test matrix of the NH_3 formation test.

Factor	Value
Lambda [λ]	0.87, 0.91, 0.93, 0.95, 0.98
Engine speed [RPM]	800, 1500, 2000, 3000
BMEP [bar]	0.5, 3, 7
TWC composition	TWC 1, TWC 2

To ensure the measurements were reliable and to reduce possible errors, the measurement sequence was standardized. Before any measurements were conducted the TWC was reconditioned at 850 °C during 30s rich and 30s lean. The selected operating point for this step was chosen to 3000rpm and 3bar BMEP. The engine was then operated at a desired engine speed and engine load. Lambda value was held at slightly lean ($\lambda = 1.02$) conditions until exhaust temperatures and emissions were stabilized. The reason to be closer to stoichiometric rather than leaner was to ensure the exhaust temperatures was closer to the corresponding temperature during the rich cycle. The data log was turned on and after 5s a step change to the rich cycle was performed. The measurements were continuously sampled until catalyst temperatures and NH_3 formation was stabilized. The continuously measurement of emissions and NH_3 were collected post TWC. In the end of the measurement cycle, the measurement position was changed to pre TWC where a sample was measured for the last 10s to determine engine out emissions. The data log was then turned off and the

measurements files were imported into Matlab for analysis. The engine was then operated at lean condition until emissions and temperatures were stabilized and the procedure was repeated for all rich steps. When all rich steps had been performed the TWC was reconditioned once again and the next operating point was chosen.

7.3.2 Ammonia formation at lambda cycling

For engines operating at stoichiometric conditions, the real lambda value is not constantly equal to one. Normally the lambda value is oscillating$\pm$ 1,5%. The purpose of this test was to investigate if any NH_3 can be formed by imitating lambda cycling and if so by how much. This was done by varying the amplitude and frequency of the cycling. The amplitude was varied equally on the rich and lean side. The cycle frequency was varied in three different steps to deplete the OSC of the TWC differently. One cycle is a lean period followed by a step change in lambda into a rich period. The test matrix can be seen in Table 8 below.

Table 8. Test matrix of the lambda cycling test.

Lambda [λ]	Cycle frequency [Hz]	Lean period [s]	Rich period [s]
0.99 – 1.01	0.1, 0.05, 0.025	5, 10, 20	5, 10, 20
0.98 – 1.02	0.25, 0.1, 0.05	2, 5, 10	2, 5, 10
0.95 – 1.05	0.1667, 0.1, 0.05	3, 5, 10	3, 5, 10

To ensure the correct lambda values were achieved during the lambda cycling test, the maximum and minimum lambda values were manually defined in VAT2000. Entering a too rich or too lean lambda value during the experiment would not cause the lambda to exceed the defined values. This enabled a simple procedure to cycle between the desired values. The data log was turned on and after 5s the cycling begun. The cycling was performed manually by counting seconds from a stopwatch and repeated for at least eight cycles or until a repetitive behavior of NH_3, λ and emissions could be recognized. The tests began and stopped at the lean side and were performed at 1500rpm and 3bar BMEP.

7.3.3 Depletion of OSC

A TWC generally has some sort of OSC. The OSC is a depot of oxygen used to oxidize CO and HC when the engine is lambda cycling into the rich side. An engine is controlled using the lambda value obtained pre the TWC because the response of the lambda value is fast at this point. When the engine is entering the rich side, the lambda value post the TWC is considerable slower and requires a period of time before a rich mixture is detected. How long the lambda value will stay at the lean side depends on the OSC. When the lambda value post the TWC is decreasing it means the mixture becomes richer and the oxygen depot being depleted. By comparing the actual lambda value pre and post the TWC it was possible to determine how fast the OSC could be depleted by operating the engine rich.

The purpose of this test was to see if and in what way the OSC was influencing the NH_3 formation. The test was carried out by operating the engine lean and switched to rich mode. The engine was switched back to lean mode when the lambda value post TWC had reached the same value as pre TWC. This was done for the same lambda amplitudes as for the previous lambda cycling test, see Table 8. The maximum and minimum lambda values were defined in the same way as in the previous lambda cycling test. The chosen operating point for this test was 1500rpm and 3bar BMEP.

7.3.4 Ammonia storage capacity and NO_x reduction efficiency

The purpose with this test was to determine the NH_3 storage capacity in the SCR catalyst for different brick temperatures when operating the engine rich. When a certain amount of NH_3 was stored, a switch to lean operation was made. The following lean period formed engine out NO_x. By comparing NO_x pre and post the SCR catalyst the NO_x reduction efficiency over the SCR catalyst could be determined. The test was performed at 1500rpm 3bar BMEP and $\lambda = 0.95$ for the rich cycle and $\lambda = 1.1$ for the lean cycle. At this operating point, NH_3 into the SCR catalyst was measured to be 750ppm. This concentration into the SCR catalyst was assumed during all tests since the FTIR only had one measuring probe. The NH_3 slip was measured with the FTIR post the SCR catalyst and thereby the amount of stored NH_3 could be calculated. To control the temperature of the exhaust gases an exhaust gas cooler was used shortly before the SCR catalyst with a manual valve to control the water flow into it.

The maximum NH_3 storage capacity was determined by operating rich until a NH_3 slip of 300ppm was measured. A switch to lean operation was then made and measurements were continued until the NO_x reduction efficiency had decayed to 0%. The NO_x was measured post the SCR catalyst and a reference value into the SCR catalyst was measured before the rich cycle started and at the end of the lean cycle. The experiment was also repeated for shorter rich periods of 250s to evaluate the NO_x reduction efficiency when no NH_3 slip was present. The test was carried out for both SCR catalysts.

8 Results

In the following chapter the results from the performed experiments are presented and analyzed. It should be noted that the measurement equipment of the emissions has different response times.

8.1 Ammonia formation steady state

The NH_3 formations during rich operation with TWC 1 are presented in Figure 20 to Figure 23. The result shows continuously measurement of NH_3 formed over the TWC. The rich step starts 5s into the cycle and as can be noticed the detection of NH_3 varies with engine speed, load and lambda. Generally it could be stated that an increased engine speed, load or decreased lambda yields a faster detection of NH_3.

Since the response time of the FTIR is slow (<120s specified from the manufacture) it is hard to analyze whether the NH_3 formation is slow or the system response is slow. In order to determine the system response a gas with known concentration was connected to the inlet probe of the FTIR. The FTIR had a response time of approximately 5s and a steady state value was obtained within 20s. This simple test showed there is a delay time of at least 5s before emissions is detected and for the following 15s the measurement accuracy of NH_3 concentration is unknown.

At high loads and high engine speeds NH_3 formation slowly increases and a steady state value cannot be observed even after 400s. This phenomenon lacks explanation. However a steady state value could be obtained after a significantly longer time span. Even though the NH_3 concentration is rather similar at some points the produced amount of NH_3 is larger with increased exhaust mass flow, hence increased load and engine speed is favorable to form larger amounts of NH_3.

800rpm and 0.5bar BMEP shows a fairly low concentration of NH_3, see Figure 20. Initially a concentration of around 100ppm is formed for the entire lambda range. Richer mixtures than $\lambda = 0.93$ result in increased concentrations to around 200ppm after 100s with fluctuating measurements. These results are only noticed on low loads and low exhaust mass flows. Increased load to 3 and 7bar BMEP shows a significantly higher concentration and the impact of mixture composition is obvious. Maximum NH_3 concentration is formed at $\lambda = 0.91 - 0.95$.

1500rpm shows similar results as for 800rpm, see Figure 21. The impacts of different lambda are negligible for 0.5bar BMEP. For higher loads NH_3 concentration is significantly higher and varies a lot with lambda.

The results at 2000rpm, see Figure 22, shows an increased NH_3 formation at 0.5bar BMEP compared to the previous lower engine speeds. At 7bar BMEP a steady state value is only obtained at the richest mixture. This indicates richer mixtures will reach a faster steady state value of NH_3 concentration.

At 3000rpm the only stable steady state value within 400s is obtained at 0.5bar BMEP. This load shows the highest concentration compared with lower engine speeds, see Figure 23. Increased load yields NH_3 formation which starts at low concentration and thereafter slowly increases with time, higher loads enhances this effect.

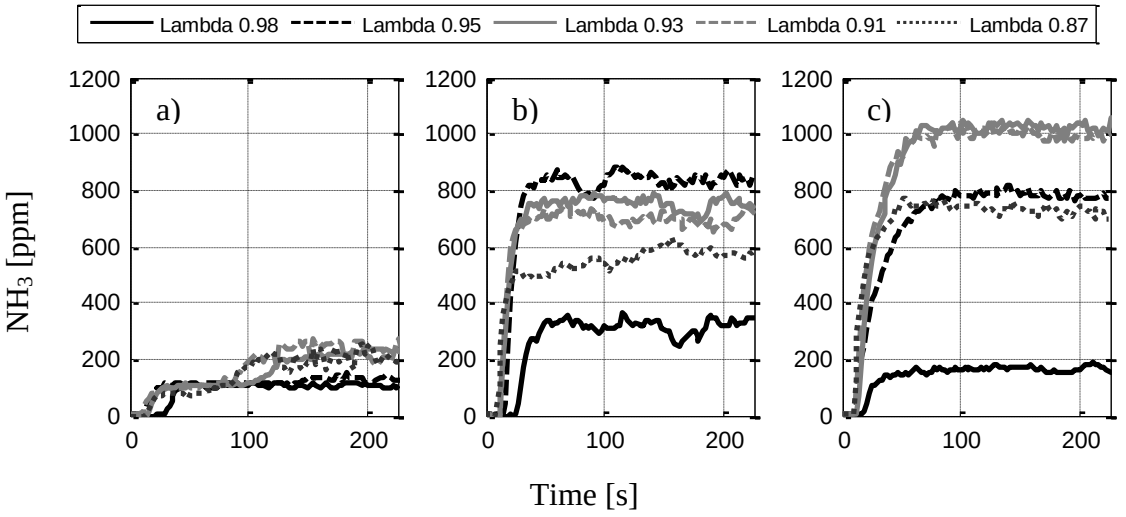

Figure 20. NH_3 formation for TWC 1 at 800rpm and at (a) 0.5bar BMEP, (b) 3bar BMEP, (c) 7bar BMEP.

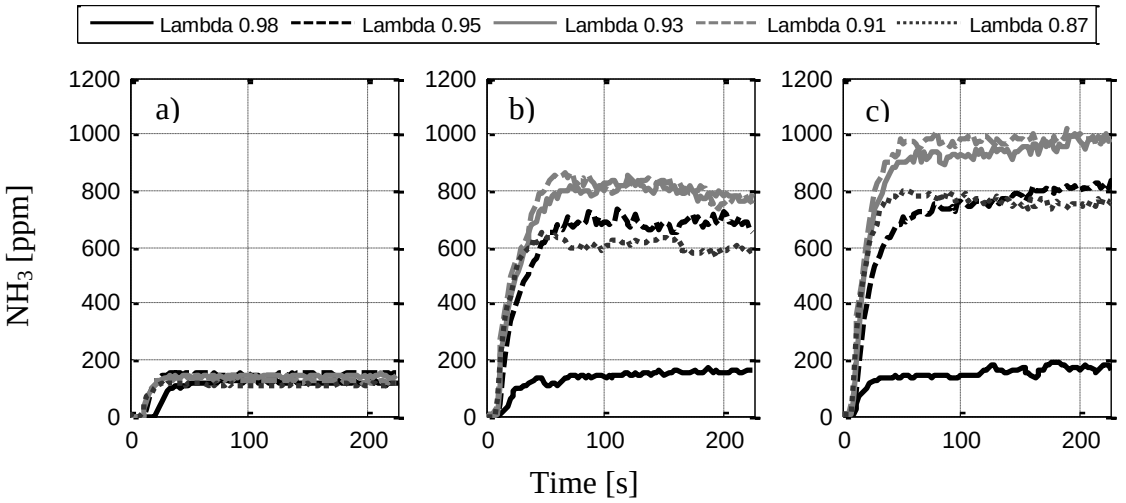

Figure 21. NH_3 formation for TWC 1 at 1500rpm and at (a) 0.5bar BMEP, (b) 3bar BMEP, (c) 7bar BMEP.

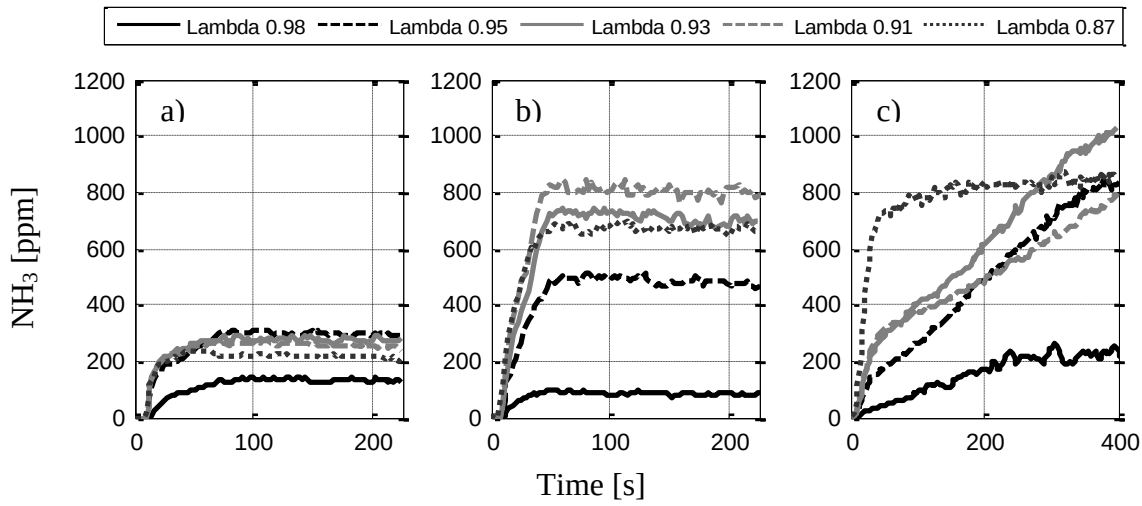

Figure 22. NH_3 formation for TWC 1 at 2000rpm and at (a) 0.5bar BMEP, (b) 3bar BMEP, (c) 7bar BMEP.

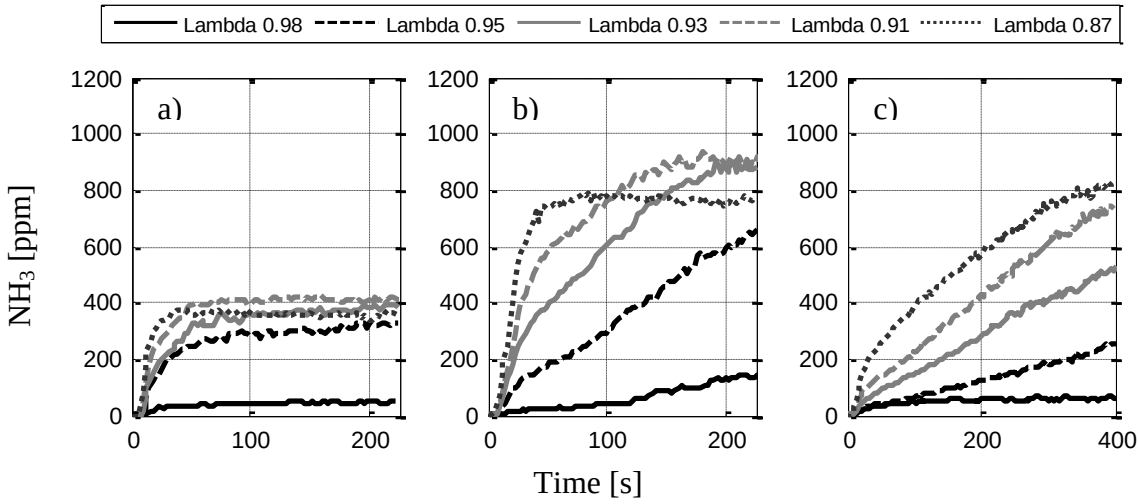

Figure 23. NH_3 formation for TWC 1 at 3000rpm and at (a) 0.5bar BMEP, (b) 3bar BMEP, (c) 7bar BMEP.

The results of the NH_3 formation for TWC 2 are presented in Figure 24 to Figure 27. The trends of the NH_3 formation is rather similar to TWC 1, except at higher loads and higher engine speeds were faster steady state values were obtained. It could also be stated that the NH_3 formations varies with load, engine speed and lambda. Generally it could be stated that at low loads the NH_3 formation distribution between different lambda values are low. Increased load increases the distribution between the formed NH_3 with respect to lambda value.

The results also show how long rich cycle duration is required until a stable steady state value is obtained. However these results are related to the response time which was stated to at least 5s. These results are therefore only useful to determine the steady state NH_3 concentration at different operating conditions, and an approximation of the transient behavior. In order to determine the transient behavior a faster FTIR should be used.

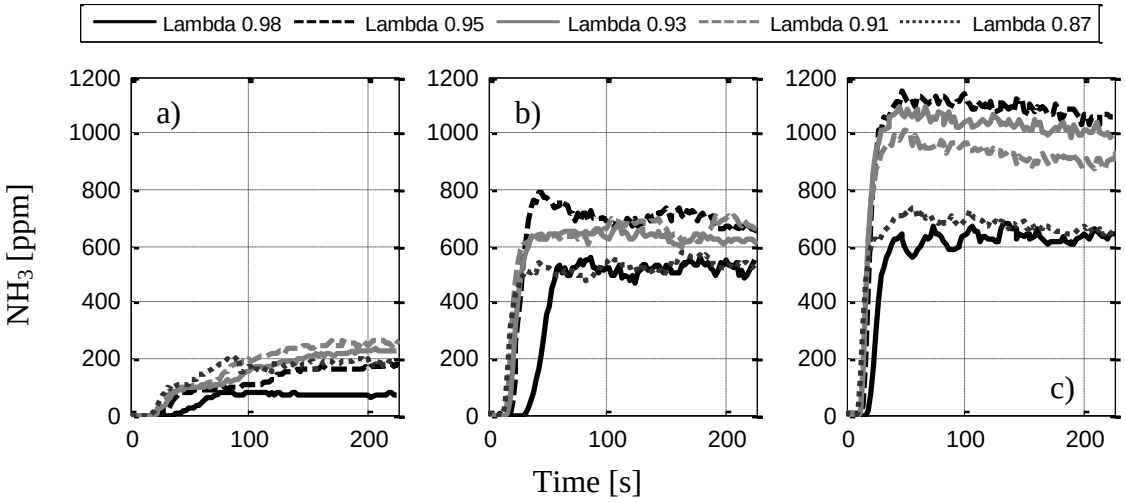

Figure 24. NH3 formation for TWC 2 at 800rpm and at (a) 0.5bar BMEP, (b) 3bar BMEP, (c) 7bar BMEP.

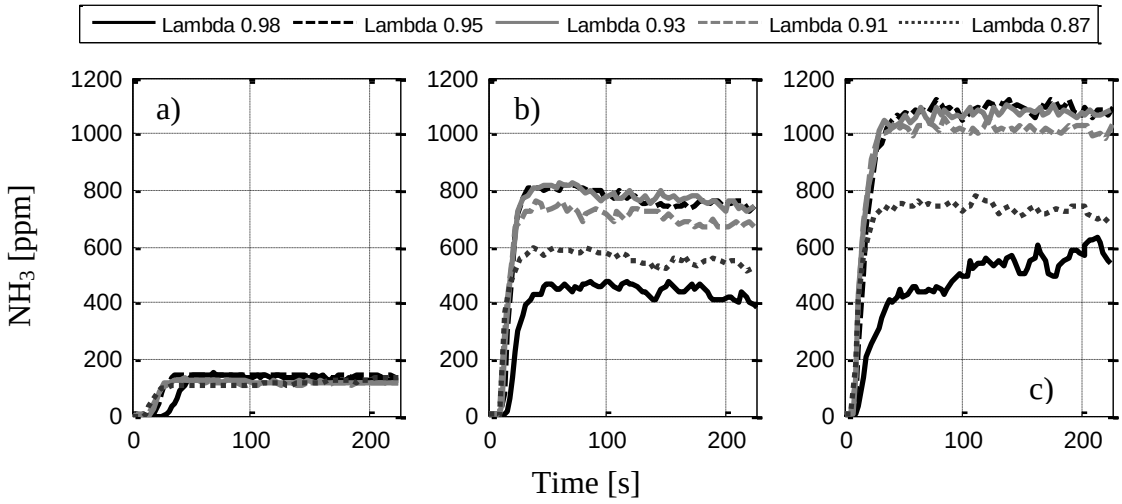

Figure 25. NH_3 formation for TWC 2 at 1500rpm and at (a) 0.5bar BMEP, (b) 3bar BMEP, (c) 7bar BMEP.

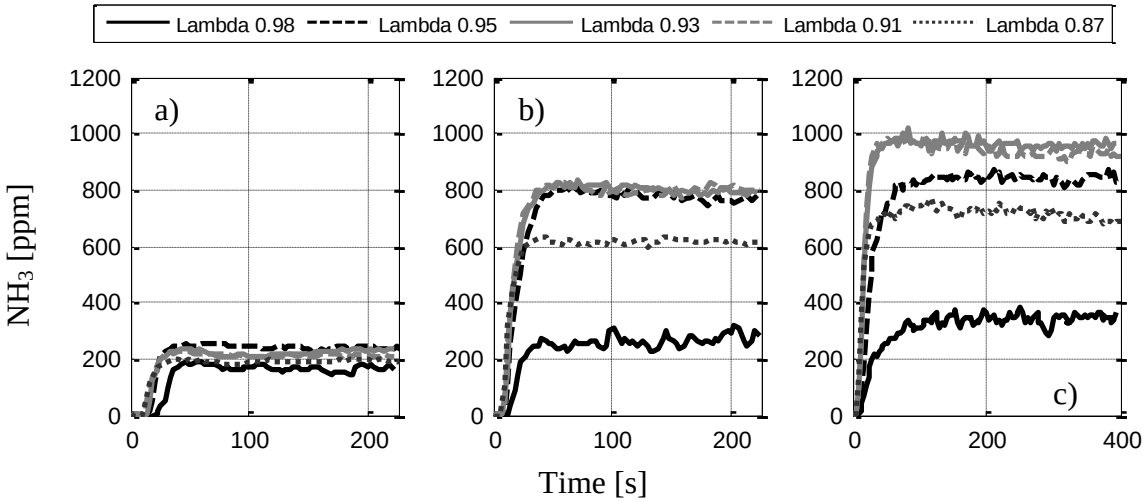

Figure 26. NH_3 formation for TWC 2 at 2000rpm and at (a) 0.5bar BMEP, (b) 3bar BMEP, (c) 7bar BMEP.

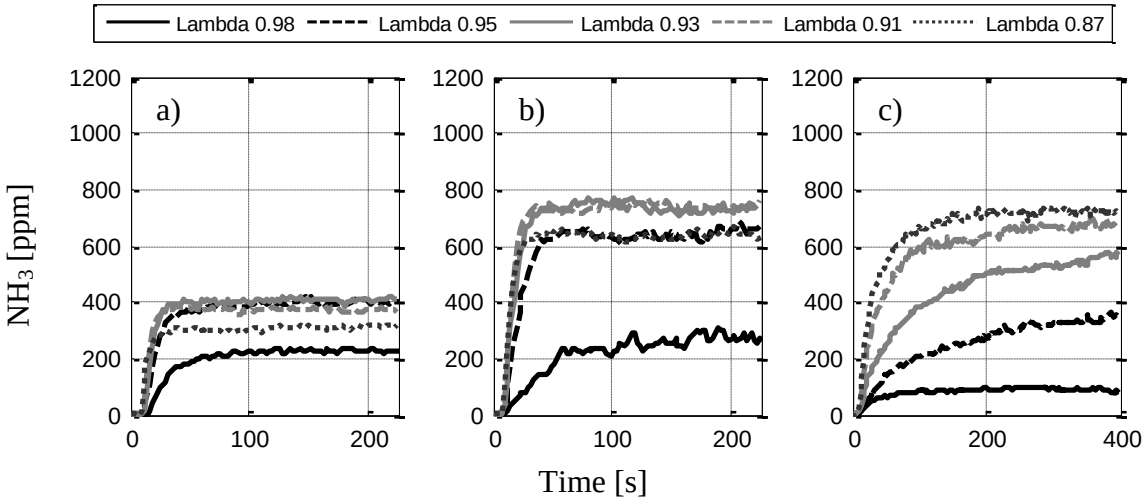

Figure 27. NH_3 formation for TWC 2 at 3000rpm and at (a) 0.5bar BMEP, (b) 3bar BMEP, (c) 7bar BMEP.

Figure 28 to Figure 31 represents the NH_3 steady state values at different engine speeds, engine loads, lambda and the two TWCs. The results are gathered from the continuously measurements and presented as the last 120s mean value. For those operating points where a steady state value could not be obtained within 400s, additional measurements were conducted until the NH_3 formation was stabilized. High concentration of NH_3 is formed at 3 and 7bar BMEP and the maximum NH_3 formation varies between $\lambda = 0.91 - 0.95$ depending on operating conditions and TWC composition. In order to achieve these stable values the engine requires to be operated at rich mixtures for at least 20s and in the extreme case up to 20 minutes. The result shows that engine load has a large impact on the NH_3 formation together with lambda value. Engine speed seems to have a small impact on the NH_3 formation, the most obvious impact of engine speed is noticed at 3000rpm compared to lower engine speeds.

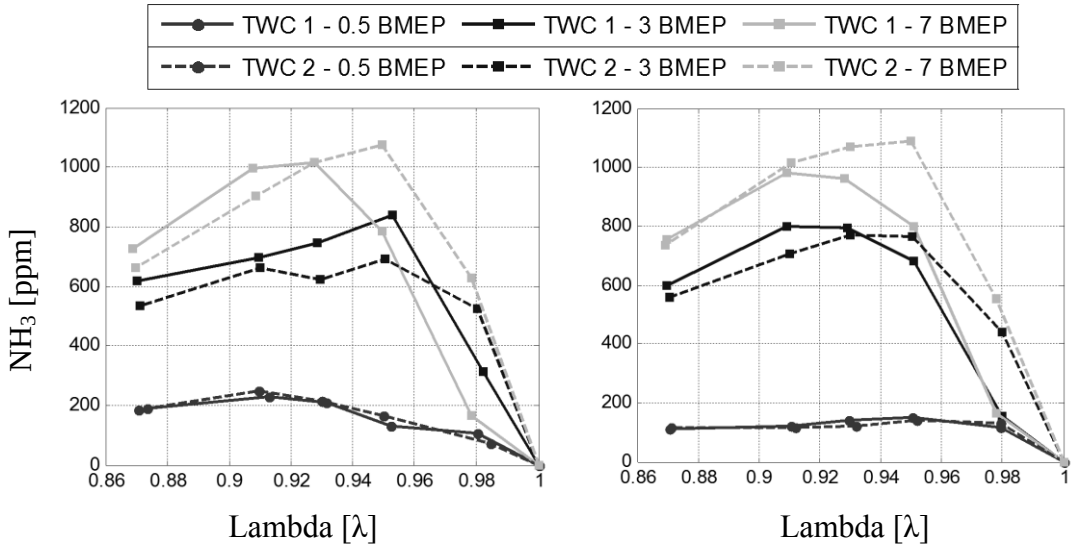

Figure 28. 800rpm steady state NH_3 formation.

Figure 29. 1500rpm steady state NH_3 formation.

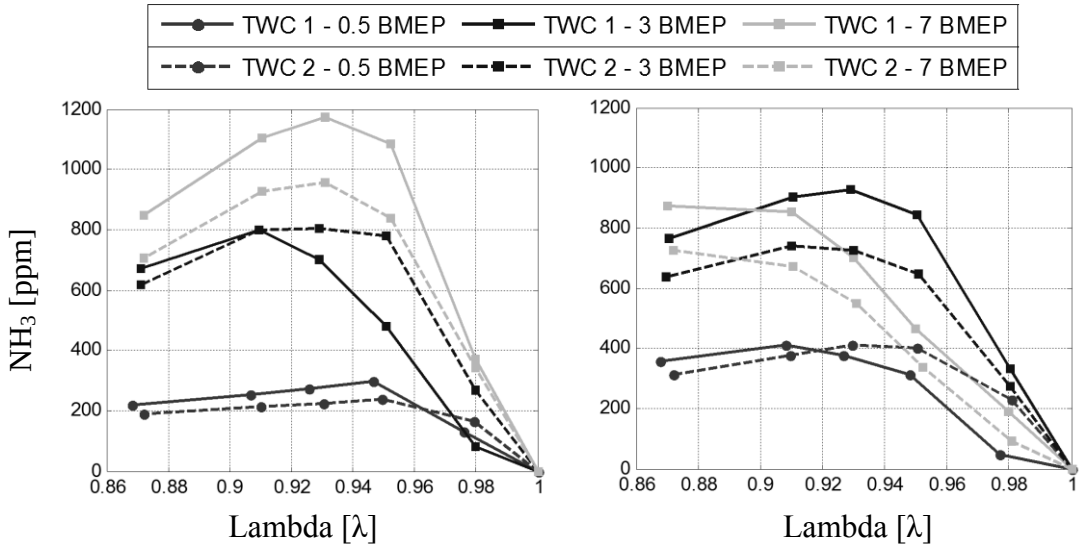

Figure 30. 2000rpm steady state NH_3 formation.

Figure 31. 3000rpm steady state NH_3 formation.

In Figure 32 and Figure 33 the steady state NH_3 formation are represented for different loads as a function of exhaust mass flow. Comparing the exhaust mass flow with regard to NH_3 formation shows the impact of PGM composition. TWC 1 indicates a maximum NH_3 formation at 20 g/s whereas TWC 2 indicates it at around 12 g/s. The major difference between the different engine loads with the same exhaust mass flow (9-10 g/s), is the concentration of NO_x at corresponding lambda, which is highest at 7bar BMEP and lowest at 0.5bar BMEP. This indicates that high NH_3 concentration is formed at high concentration of engine out NO_x. By approaching a stoichiometric mixture result in decreasing CO and increasing NO_x, hence NH_3 formation decreases. This could probably be explained by decreased level of CO or possible H_2 which limits the formation according to theory.

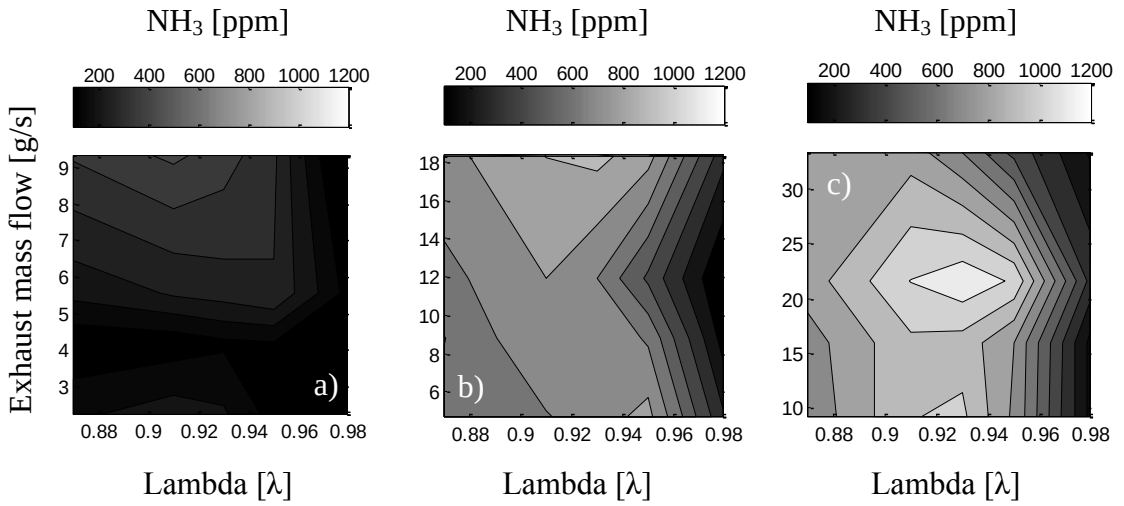

Figure 32. NH_3 formation for TWC1 at a) 0.5bar BMEP, b) 3bar BMEP c) 7bar BMEP.

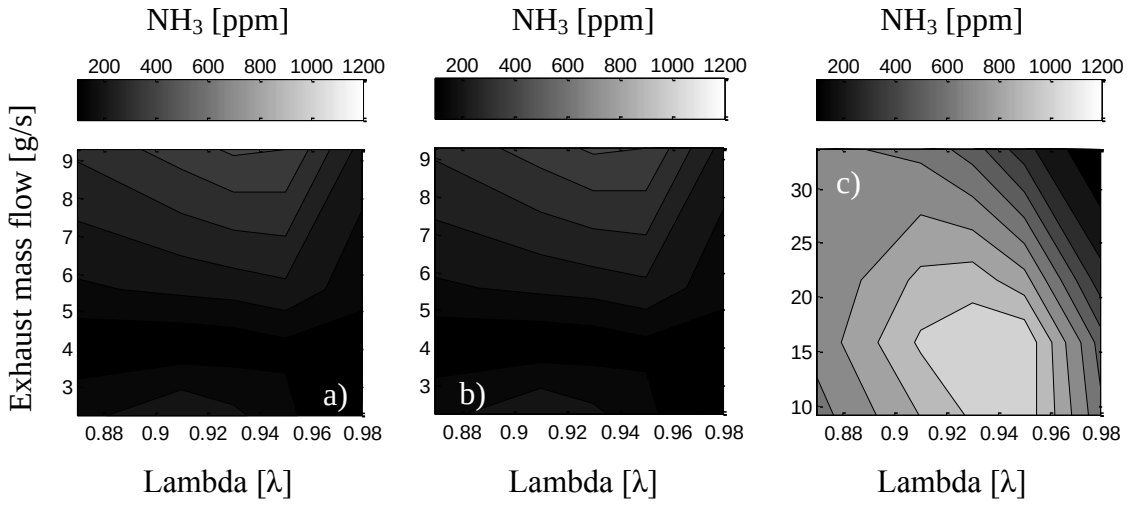

Figure 33. NH_3 formation for TWC2 at a) 0.5bar BMEP, b) 3bar BMEP c) 7bar BMEP.

Figure 34 and Figure 35 shows the NH_3 formation for both TWC catalysts as a function of engine out NO_x and CO emissions. The result shows that in order to form NH_3, both NO_x and CO is required. High concentration of NH_3 is formed when high concentrations of both NO_x and CO are present. However a to low concentration of either NO_x or CO seems to limit the NH_3 formation. It could be noticed that some points shows a significantly lower concentration of NH_3 compared to points close to the equivalent CO and NO_x concentration. By comparing the exhaust gas temperature and the exhaust mass flow for these points it shows that the majority of points with significantly lower NH_3 formation have significantly higher exhaust gas temperature and exhaust mass flow.

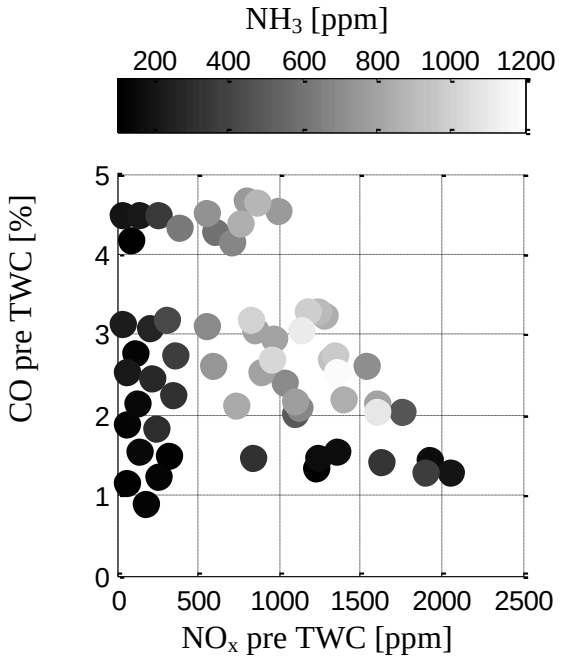

Figure 34. NH_3 formation for TWC1 as a function of engine out NO_x and CO.

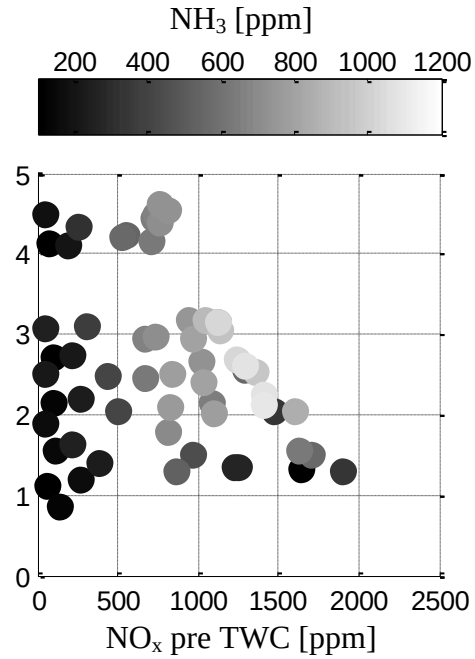

Figure 35. NH_3 formation for TWC2 as a function of engine out NO_x and CO

8.2 Ammonia formation at lambda cycling

The results from the lambda cycling experiments are presented in Figure 36 to Figure 38. All emissions are measured after the TWC unless otherwise stated.

Figure 36 shows lambda cycling between $\lambda = 0.99 - 1.01$. It is noticed for TWC 1 and TWC 2 that NH_3 is only formed for the longest cycle duration of 0.025 Hz, however the amount is small and can be considered negligible. The amount of NH_3 is approximately the same for both TWCs but with the difference that the amount of CO is considerably higher for TWC 1. The increased level of CO is probably due to that the OSC is depleted earlier for TWC 1 and lacks stored O_2 to oxidize engine out CO.

For 0.025 Hz the CO level is considerably lower for TWC 2, but instead the peaks of engine out NO_x are higher. The engine out NO_x increases faster for this frequency compared to TWC 1. However for the other two frequencies the peak concentrations are less. None of the TWCs reduces NO_x satisfactory but TWC 2 seems best suited for transient lambda cycling to reduce CO and NO_x for this lambda amplitude. No considerable amounts of NH_3 were formed for either of the TWCs.

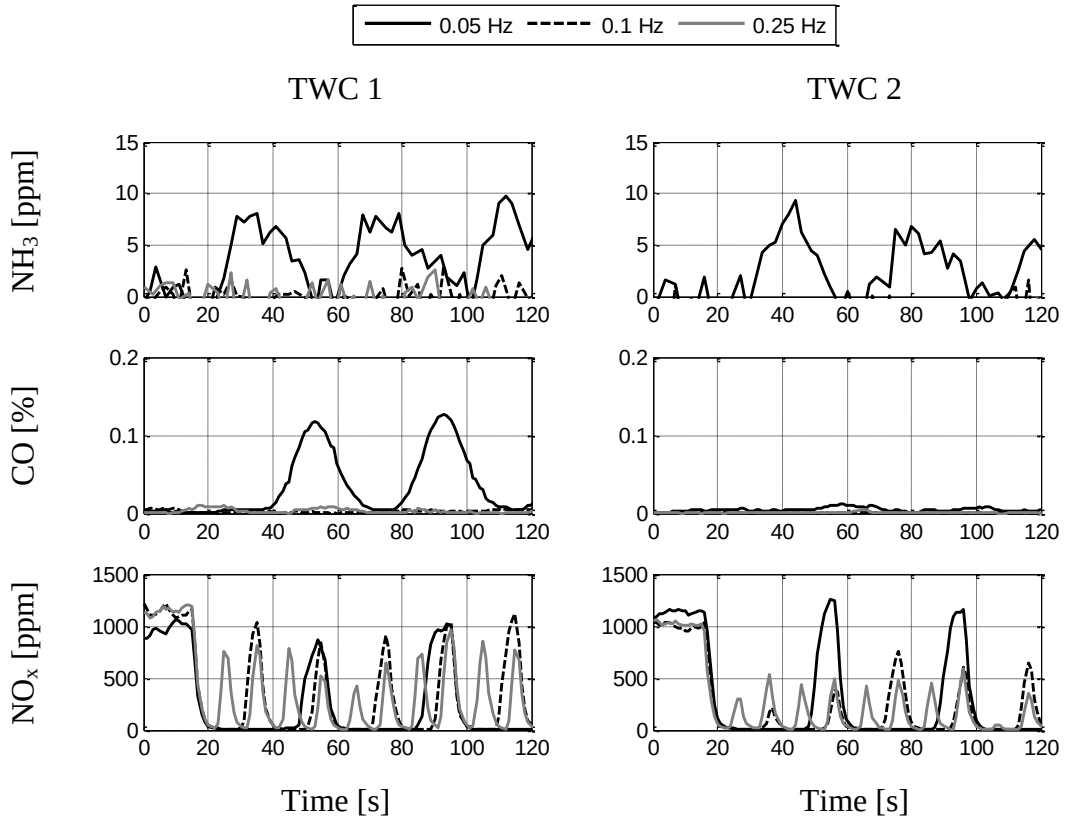

Figure 36. Lambda cycling 0.99-1.01 at 1500rpm 3bar BMEP.

Figure 37 shows lambda cycling between λ = 0.98 - 1.02. At this amplitude, the cycle frequencies have been increased due to that the OSC is depleted earlier for a richer mixture.

It is noticed for TWC 1 that the amount of CO is slightly increased for the cycle frequencies of 0.05 and 0.1 Hz compared to the previous amplitude. It also shows a small increment of NH_3 is obtained for each frequency. There seems to be a relation between CO and NH_3, when CO post TWC increases in the exhaust gas so is also NH_3. As for TWC 2 the levels of CO are approximately the same compared to the previous amplitude. This is probably due to that none of the frequencies are sufficient to deplete the OSC and therefore no significantly amount of NH_3 is formed.

It can be seen for TWC 1 and 0.05 Hz that high peaks of engine out NO_x is detected, this is probably due to the frequency is relative low which results in long dwell times at the lean side. For the other frequencies the dwell time of lean operation is shorter which results in high NO_x reduction efficiency. This applies for TWC 2 for all frequencies as well, even if the reduction for 0.25 and 0.05 Hz is not as high as for 0.1 Hz. This behavior can probably be explained by that lambda is pending close to λ = 1 at a satisfactory frequency. This test shows the importance of correct cycling frequency to reduce and oxidize emissions at stoichiometric conditions on a TWC.

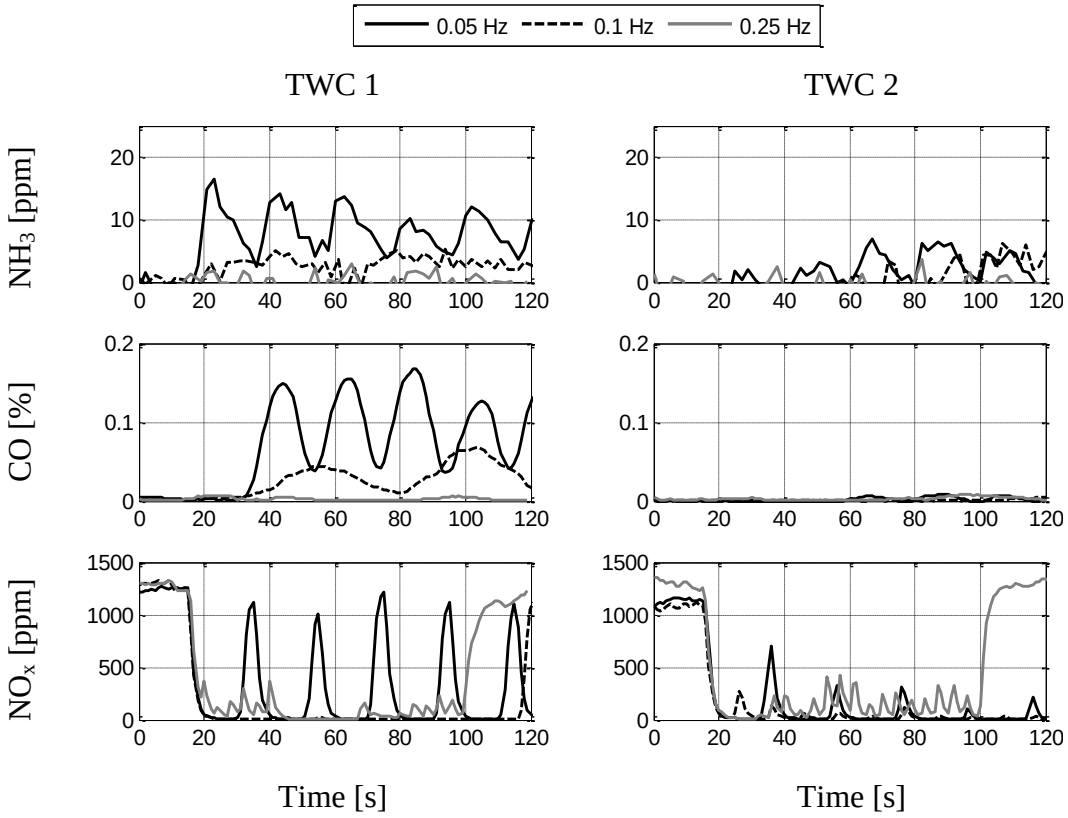

Figure 37. Lambda cycling 0.98-1.02 at 1500rpm 3bar BMEP.

Figure 38 shows lambda cycling between λ = 0.95 - 1.05. At this lambda amplitude depletion of the OSC is very fast. Compared to the previous amplitude the frequencies are kept the same except for the highest frequency which is decreased.

At this amplitude CO is detected for all frequencies except at 0.1667 Hz for TWC 2. At the same time as CO increases so is also NH_3 for these frequencies. For both TWCs it is noticed that a longer dwell time on the rich side results in increased NH_3 formation. It was concluded previously that TWC 2 probably has a larger OSC and would therefore experience a shorter rich dwell since it has a larger O_2 buffer to deplete. However at 0.05 Hz it clearly shows that the amount of NH_3 formed at TWC 2 is greater than TWC 1 even though the actual time at the rich side is shorter. It could therefore be stated that TWC 1 forms NH_3 earlier but as soon as the OSC is depleted for TWC 2 the NH_3 formation is larger.

The amount of CO at 0.05 Hz is larger for TWC 1, however the NH_3 formation is greater for TWC 2. The result indicates that the PGM composition in TWC 2 has a greater potential to form more NH_3 and is more favorable as CO emissions is reduced compared to TWC 1.

The NO_x reduction is almost 100 % at 0.1667 Hz for TWC 1 and at 0.1 and 0.1667 Hz for TWC 2. This is probably due to that lambda is pending close to λ = 1 at a satisfactory frequency.

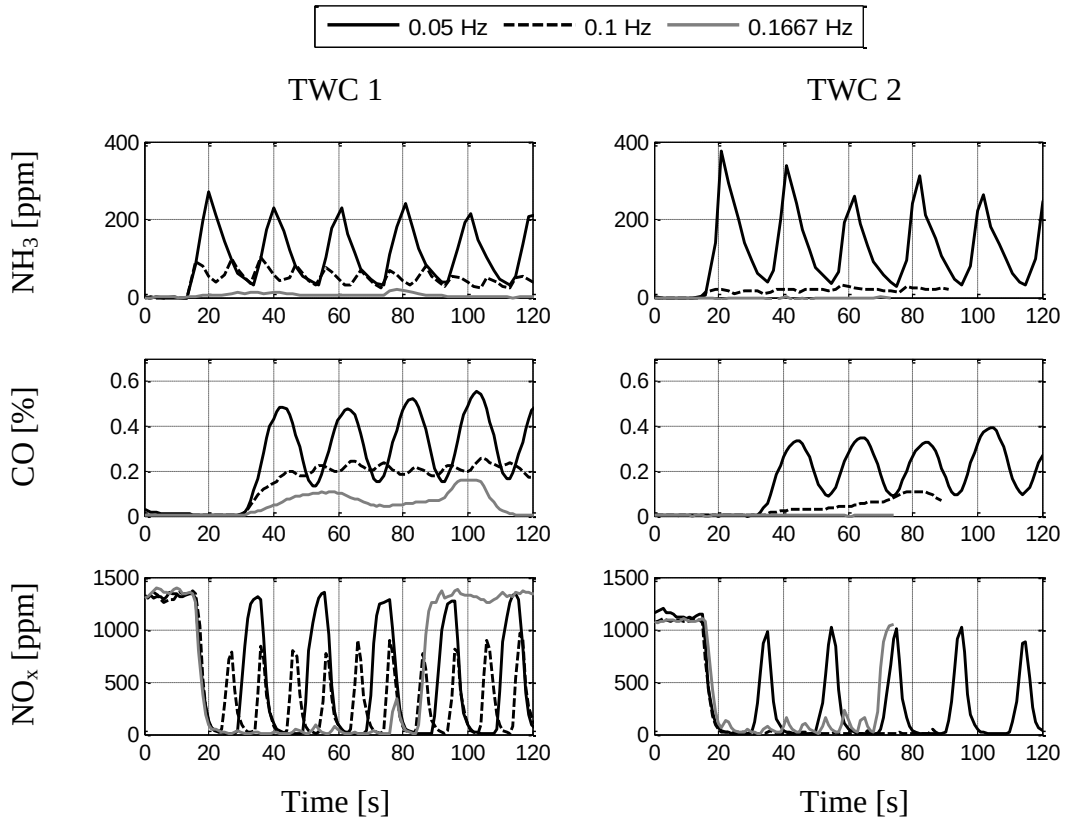

Figure 38. Lambda cycling 0.95-1.05 at 1500rpm 3bar BMEP.

8.3 Depletion of OSC

Figure 39 shows the results from the OSC depletion test. The results are obvious, it takes a shorter period of time to deplete the OSC for a richer lambda step. This is due to that the engine is producing a lot more CO and HC which needs to be oxidized. It is also noticeable that no NH_3 is formed until lambda post TWC has decreased below $\lambda = 1$. This confirms the behavior seen earlier that no NH_3 forms unless CO is detected post TWC. It can be noticed that approximately the same amount of CO is formed for both TWCs at $\lambda = 0.98 - 1.02$, however a significantly larger amount of NH_3 is formed. It could be noticed for TWC 2 that at richer lambda steps significantly more NH_3 is formed compared to CO. An error occurred during the richest step for TWC 1, and therefore the switch back to lean when lambda post TWC had reached the target was delayed. This delay makes it difficult to compare the results for the richest step. The OSC depletion test shows that TWC 2 has a larger OSC since it takes a longer time until lambda post TWC decreases below $\lambda = 1$, especially for the less rich lambda step.

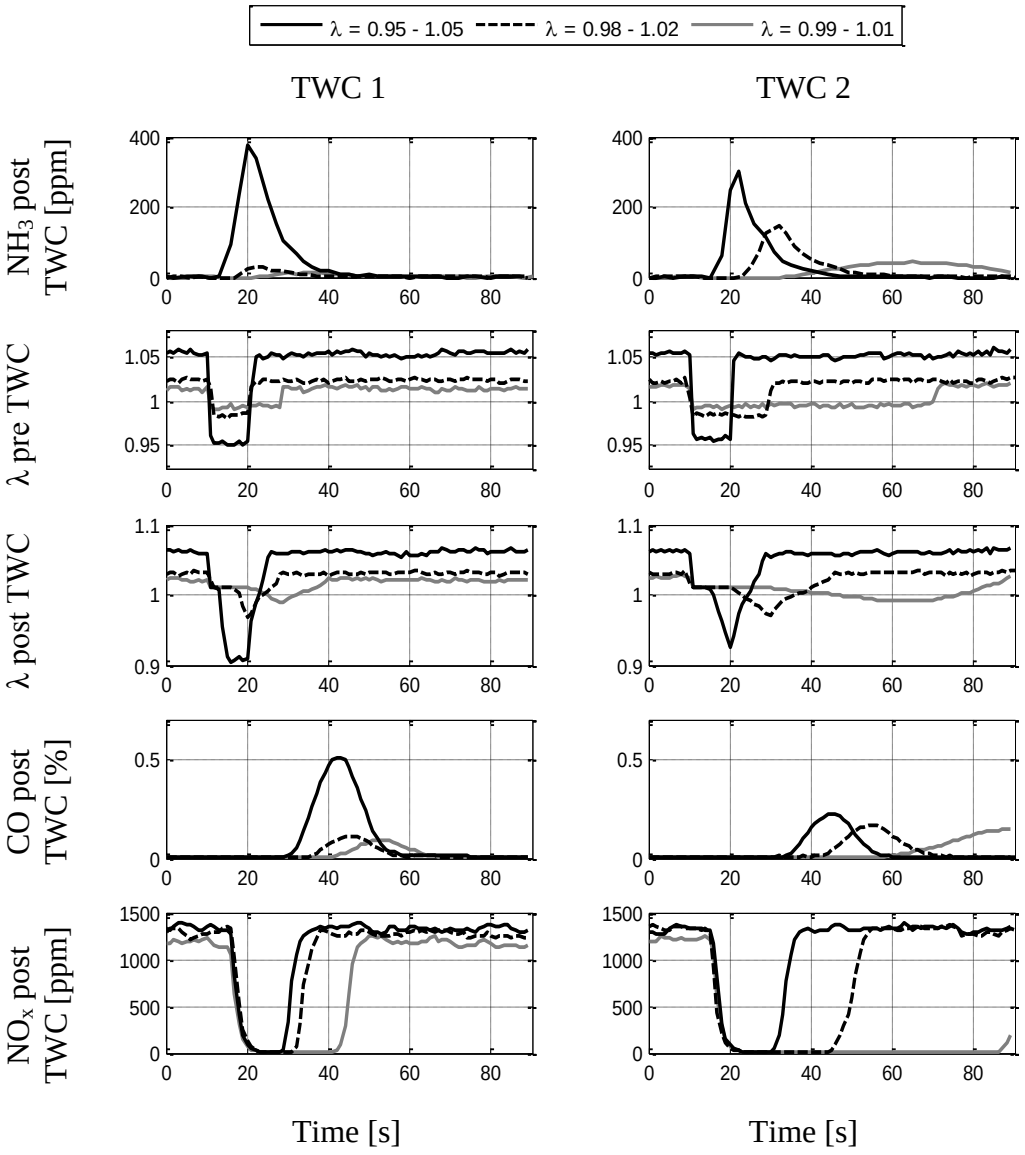

Figure 39. OSC depletion test at 1500rpm and 3bar BMEP.

8.4 Ammonia storage capacity and NO_x reduction efficiency

The NH_3 storage capacity was determined by operating the engine rich at λ = 0.95, 1500rpm and at 3bar BMEP. The results from the experiment are showed in Figure 40 for SCR 1. The SCR catalyst brick temperature is represented for both the rich and the lean cycle for each test in the legend on top of the figure. Within the parenthesis the temperature during rich is stated to the left and the temperature during lean to the right.

As the SCR catalyst is filled with NH_3 only negligible NH_3 slip occur. When a certain amount of NH_3 has been stored it could be noticed that the NH_3 slip increases exponentially. The result shows that NH_3 is released from the SCR catalyst even after the switch to lean operation. This could be explained by the temperature increasing due to leaner mixtures. Generally it could be noticed a brick temperature increment of 10 °C occurred after the switch to lean operation. It could be stated from the results that the storage capacity decreases with increasing temperature since it take less time to fill the SCR catalyst at higher temperatures.

A 100% NO_x reduction efficiency could be seen for all brick temperatures after the switch to lean operation. Subsequently NO_x increases slowly until all NH_3 is depleted in the SCR catalyst. Noticeable are the gradient of NO_x reduction efficiency which decays faster with increasing temperatures.

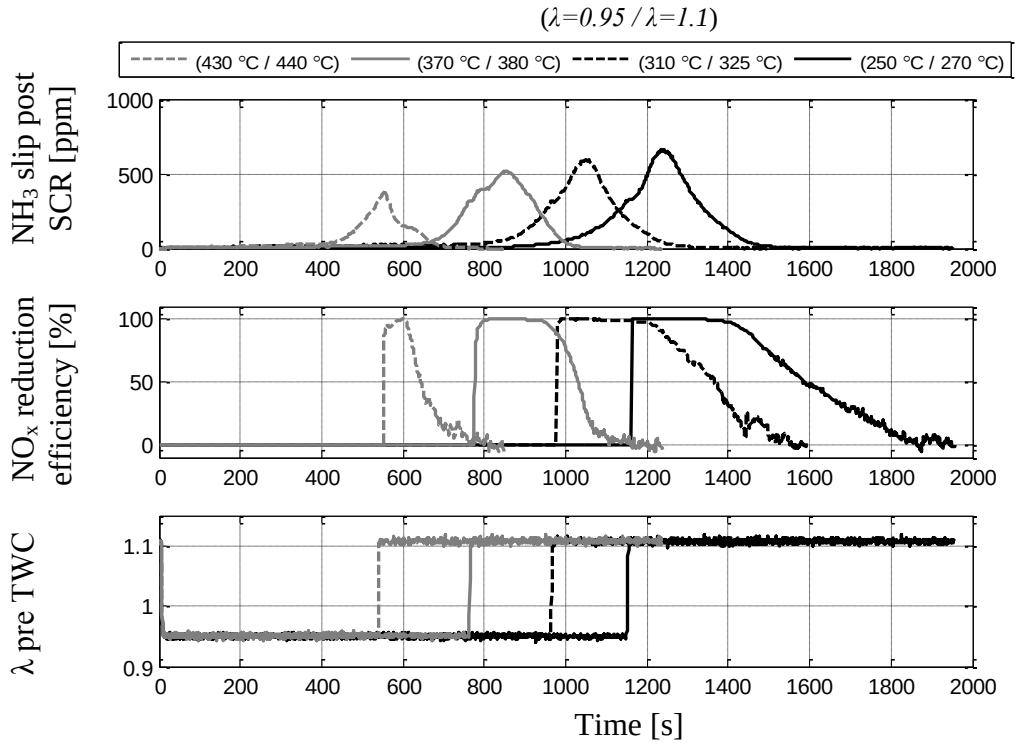

Figure 40. NH_3 storage capacity test and NO_x reduction at 1500rpm and 3bar BMEP for SCR 1.

Figure 41 shows the results for the second SCR catalyst. It shows the same behavior as the first SCR catalyst. Since SCR 2 has a larger volume it requires a longer rich period to fill the SCR catalyst.

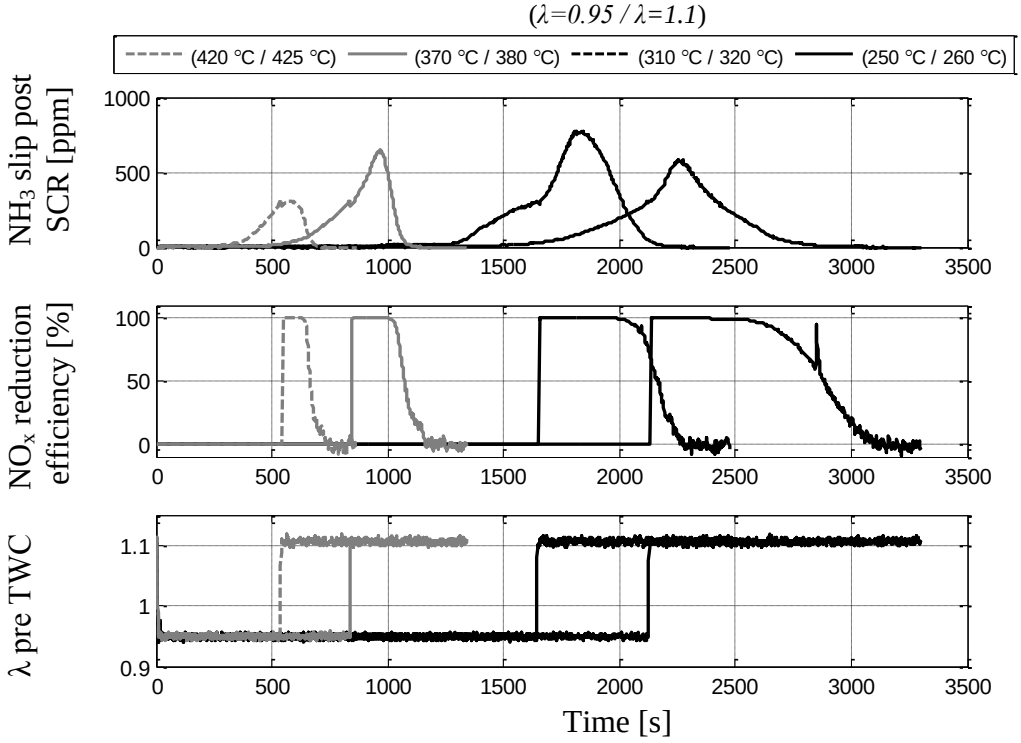

Figure 41. NH_3 storage capacity test and NO_x reduction at 1500rpm and 3bar BMEP for SCR 2.

The NH_3 storage capacity at different brick temperatures are showed in Figure 42 for both SCR catalysts. The result is based on the assumption that the SCR catalysts are filled with NH_3 until an NH_3 slip of 300ppm is detected. The result shows that the NH_3 storage capacity is significantly larger for SCR 2 at lower temperature however SCR 1 has a larger storage capacity at higher temperatures. It could be seen for both SCR catalysts that increased temperatures reduces the NH_3 storage capacity which corresponds to the expected result according to theory in chapter 5.

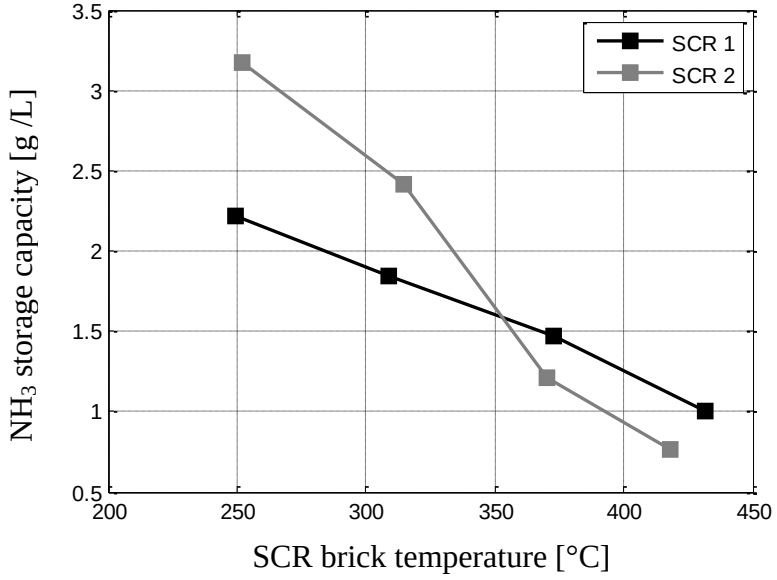

Figure 42. SCR NH_3 storage capacity for different brick temperatures.

The NO_x reduction efficiency when NH_3 slip occurred was 100% initially. The NH_3 slip may affect the NO_x reduction efficiency and the long rich duration is not a realistic operating condition. Tests with shorter rich cycle duration were therefore conducted, when no NH_3 slip was observed. The rich cycle was set to 250s whereas a lean period followed until NO_x reduction efficiency had decayed to 0%.

Figure 43 shows the result from the experiment for SCR 1. A negligible NH_3 slip was detected during the rich cycle. The only difference between the series of tests was the brick temperature on the SCR catalyst.

As can be seen the NO_x reduction efficiency varies a lot with brick temperature. As the temperature increases, the NO_x reduction efficiency increases. It can also be noticed that the NH_3 depletes faster at higher temperatures and thereby the NO_x reduction efficiency decays faster.

Figure 44 shows the NO_x reduction efficiency for SCR 2. The same type of behavior is seen as for SCR 1. At higher brick temperatures the NO_x reduction efficiency increases. SCR 2 has higher efficiency compared to SCR 1 at the same brick temperature. Noticeable is that the highest brick temperature (440 °C) result in a shorter NO_x reduction period compared to the brick temperature at (385 °C). This could possibly be explained by NH_3 being decomposed at higher temperatures. From the results it can also be noticed that at lower temperatures the NO_x reduction efficiency is initially high and thereafter decreases slowly.

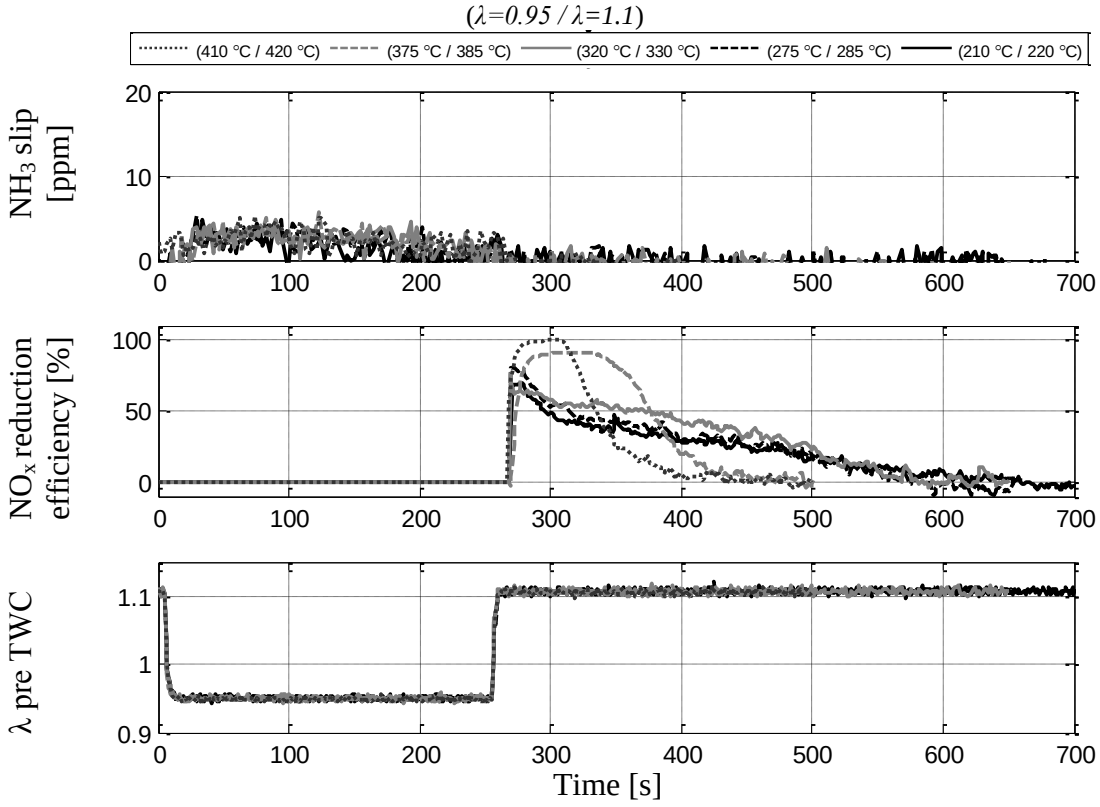

Figure 43. NO_x reduction efficiency for SCR 1 at 1500rpm and 3bar BMEP.

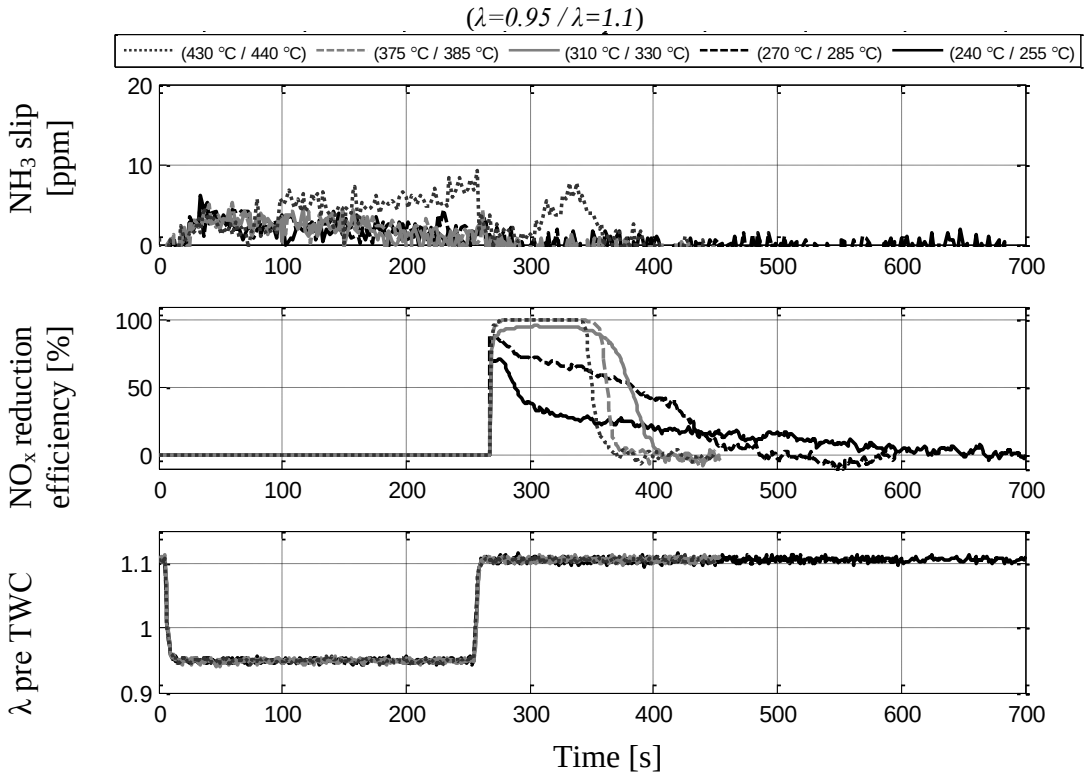

Figure 44. NO_x reduction efficiency for SCR 2 at 1500rpm and 3 BMEP.

Figure 45 summarizes the NO_x reduction efficiency for both SCR catalysts. The corresponding efficiency is collected at approximately 300s into the measuring sequence, where the NO_x reduction efficiency can be assumed to be stable. It can be seen that SCR 2 shows a better NO_x reduction efficiency for all tested brick temperatures.

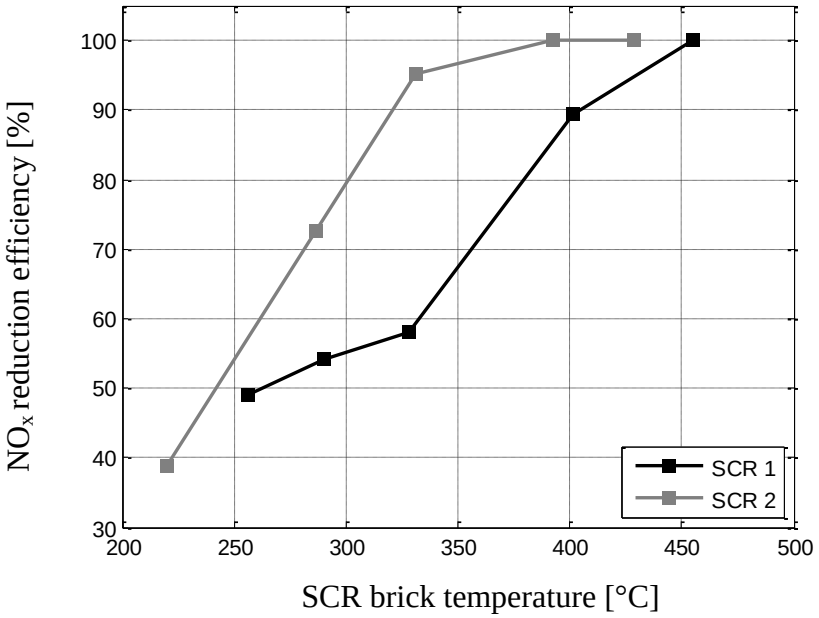

Figure 45. SCR NO_x reduction efficiency at 1500rpm and 3bar BMEP.

According to the theory in chapter 4.4 the molar ratio between NH_3 to NO should be 1:1. This means that the amount of stored NH_3 molecules in the SCR catalyst should reduce an equal amount of NO molecules, one NH_3 reduces one NO. The NH_3 storage and reduction tests show a NH_3 to NO molar ratio around 1.2:1 for the majority of the experiments. At higher temperatures it was seen that the ratio increased up to 2:1 and it was probably due to decomposition of NH_3.

Figure 46 shows the result from the system functionality by lambda cycling between λ = 0.95 - 1.05 with a frequency of 0.1Hz at 1500rpm and 3bar BMEP. The cycling was performed for 250s, thereafter a lean period at λ = 1.05 followed. A low concentration of NH_3 was formed, around 8ppm mean value. The experiment was performed twice with the same procedure to be able to measure both NO_x pre and post the SCR catalyst. The result shows that there is a time delay of approximately one second (at 275s) until NO_x post the SCR catalyst rises in concentration compared to pre the SCR catalyst. Even though this corresponds to a NH_3 to NO molar ratio of approximately 1:1 the time delay could also be a measurement error. In order to reduce NO_x significantly larger amounts of formed NH_3 are required in order to operate lean and meanwhile reducing NO_x emissions.

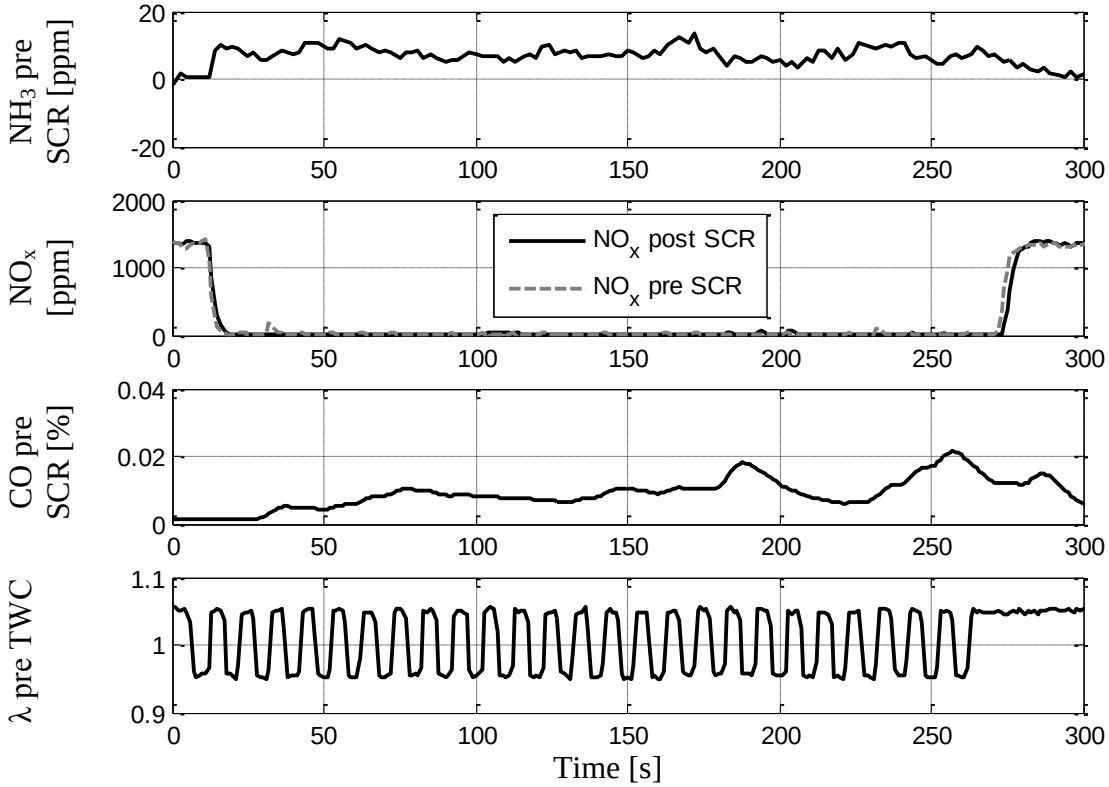

Figure 46. Lambda cycling at 0.1Hz, 1500rpm and 3bar BMEP.

9 Conclusions

It can be stated that NH_3 can be formed over a TWC by operating the engine rich. Maximum NH_3 formation for the tested TWCs showed to be at approximately λ = 0.93. The formation of NH_3 until a steady state value was obtained varied with operating conditions. The rich cycle duration was therefore of great significance. The most contributing factors to NH_3 formation are lambda and engine load. Higher load generally forms a higher concentration of NH_3 until a certain exhaust mass flow is obtained.

From the lambda cycling experiments it can be concluded that the selection of PGM composition and OSC is of importance, as it influences how much NH_3 that can be formed at different operating conditions. It could be stated that a low amount of OSC yields an earlier formation of NH_3.

In the OSC experiment the result is similar to the lambda cycling experiment. The main conclusion of this test is that no NH_3 is formed as long as there is O_2 available in the OSC. An additional conclusion can be made; when NH_3 is formed an increased level of CO is detected post TWC. This is due to lack of O_2 to oxidize CO. This can be confirmed since NH_3 was formed when lambda post TWC decreased below stoichiometric conditions when the OSC was depleted.

The NH_3 storage capacity in the SCR catalysts was affected to a great extent by the brick temperature. Temperatures between 250 - 430 °C were experimentally tested and it can be stated that with a decreasing brick temperature, the NH_3 storage capacity increases.

The SCR catalysts NO_x reduction efficiency was analyzed with regard to brick temperature. It was proven that a possible NO_x reduction efficiency of up to 100% was possible for high temperatures for both tested SCR catalysts. The efficiency showed to decrease with decreasing brick temperature. When NH_3 slip occurred from the SCR catalysts a NO_x reduction efficiency of 100% for all tested brick temperatures could be obtained.

It can be concluded that there is a tradeoff between NH_3 storage capacity and NO_x reduction efficiency. Increased temperature promotes NO_x reduction efficiency and demotes NH_3 storage capacity and vice versa.

The passive SCR concept is a possible exhaust aftertreatment system for NO_x reduction. The formed NH_3 can be stored further down the exhaust system in a SCR catalyst. By operating lean, the formed NO_x can be reduced until NH_3 is depleted. Even though this system enables NO_x reduction during lean operation, the large quantities of CO post TWC that follows NH_3 formation is unacceptable. It must be possible to form large amounts of NH_3 without excessive CO emissions in order to use the passive SCR concept as a possible exhaust aftertreatment system.

10 Future work and recommendations

For further evaluation in this field the recommendations are first and foremost to have a closer look at the substrate of both the TWC and SCR catalyst. It would be interesting to further investigate how the composition of the substrate affects NH_3 formation. From the results, NH_3 and CO seemed to be strongly related as it was almost impossible to form any larger concentrations of NH_3 without increased concentrations of CO post TWC. It would therefore be of interest to investigate which PGM materials are the most favorable for NH_3 formation. If this could be determined it would probably be possible to customize the composition and maybe achieve a TWC substrate which could form NH_3 and still oxidize CO for short periods.

From the results it was noticed that the reduction efficiency of NO_x gradually decayed, from this a hypothesis was made; that NH_3 was locally depleted over the substrate. Perhaps this could be affected by changing the geometry of the SCR substrate, maybe a more elongated design would be more beneficial.

Another interesting approach would be to look at the effect of using multiple TWCs with different OSC. For example one TWC forms NH_3 and another one oxidizes CO while letting NH_3 through.

The tests in this project were only carried out for steady state behavior. It would be interesting to investigate the NH_3 dynamics for transient behavior. Perhaps there are beneficial behaviors which could be used that are not present at steady state.

As for the measurement equipment, it would have been good to have an operational HC instrument to be able to see possible relations between NH_3 and HC. According to theory, NH_3 formation is related to engine out H_2, it would therefore be of interest to measure. With the current FTIR equipment it was noticed that the highest sampling frequency possible was 0.33 Hz with a slow response time. Therefore it would also be recommended to measure NH_3 with a higher sampling rate and faster response time. With an instrument with high sampling rate and fast response time it would be possible to see the dynamics of the NH_3 formation for short rich cycle durations. This would be useful if any further lambda cycling experiments are conducted.

11 References

[1] Zhao, F, Lai, M.C; Harrington ,D.L (1999),Automotive spark-ignited direct-injection gasoline engine, *Progress in energy and combustion science*, vol 25, nr 5, ss. 437-562

[2] Evans, R, L (2008), Lean-Burn spark-ignited internal combustion engines. *Lean combustion: Technology and control*, red. DD. Rankin, ss. 95-120. Boston: Academic Press

[3] Bosch, R (2008), Automotive Handbook, Germany: Bentley Publisher

[4] Heywood, J. B, (1998), Internal combustion engines fundamentals, McGraw-Hill Higher Education

[5] Hochgreb, S (2002), Combustion-related emissions in a SI engine. *Handbook of air pollution prevention and control*, red. N.P. Cheremisinof, ss. 119-164. Woburn: Elsevier Science

[6] Trafikverket (2010) *Handbok för vägtrafikens luftföroreningar*. http://www.trafikverket.se

[7] Ertl, G., Knözinger, H., Weitkamp, J. (1997): Preparation of Solid Catalysts. *Handbook of Heterogeneous Catalysis,* Vol. 1 No. 2 1997 pp. 49-425

[8] Ertl, G., Knözinger, H., Weitkamp, J. (1997): Reaction Engineering. *Handbook of Heterogeneous Catalysis,* Vol. 3 No. 10 1997 pp. 1399-1489

[9] Dieselnet - Online information service on clean diesel engines and diesel emissions (2011) *Catalytic Coating and Materials* http://www.dieselnet.com (27 January 2011)

[10] Association for Emissions Controls by Catalyst (2011) *Three-way catalysts* http://www.aecc.eu (11 January 2011)

[11] Ertl, G., Knözinger, H., Weitkamp, J. (1997): Environmental Catalysis. *Handbook of Heterogeneous Catalysis,* Vol. 4 No. 1 1997 pp. 1559-1697

[12] Parks II, J. et al., (2007), *Lean NOx Trap Catalysis for Lean Natural Gas Engine Applications.* Oak Ridge National Laboratory, Publication no. 1883-S821-A1, Oak Ridge, United States, 80 pp.

[13] Lifeng, X., Graham, G., McCabe R., (2007), A NOx trap for low-temperature lean-burn-engine applications. *Catalysis Letters,* Vol 115 Nos. 3-4, 2007, pp. 108-113

[14] Tagliaferri, S., Köppel, R. A., Baiker, A., (1998) Comparitive behavior of standard Pt/Rh and newly developed Pd-only and Pd/Rh Three-Way catalysts under dynamic operation of hybrid vehicles. *Studies in Surface Science and Catalysis,* Vol. 116, 1998, pp. 61-71

[15] Chang, H. K, et al., (2010) *2010 DEER Conference: Catalyst design for Urea-less Passive Ammonia SCR Lean-Burn SIDI Aftertreatment system* 28 September, 2010, Detroit.

[16] Dieselnet - Online information service on clean diesel engines and diesel emissions (2011) *Selective Catalytic Reduction*
http://www.dieselnet.com (15 February 2011)

[17] Ertl, G., Knözinger, H., Weitkamp, J. (1997): Environmental Catalysis. *Handbook of Heterogeneous Catalysis,* Vol. 4 No. 1 1997 pp. 1636-1658

[18] Ertl, G., Knözinger, H., Weitkamp, J. (1997): Deactivation and Regeneration. *Handbook of Heterogeneous Catalysis,* Vol. 3 No. 7 1997 pp. 1263-1283.

[19] Mejia-Centeno, I.; Fuentes, G. A. *Increased NH_3 and N_2O emissions from three-way catalytic converters.* Department of Process Engineering, Publication no. P-S4-23A, Iztapalapa, Mexico, 1 pp.

[20] Mejia-Centeno, I. et al., Effect of low-sulfur fuel upon NH_3 and N_2O emission during operation of commercial three-way catalytic converters. *Topics in Catalysis,* Vols. 42-43, 2007, pp. 381-385.

[21] Kodama, Y., Wong, V. W. (2010) Study of onboard NH3 generation for SCR operation. *SAE International Journal of Fuel and Lubricants,* Vol. 3 No. 1 August 2010 pp. 537-555.

[22] Wei, Li,. et al. (2010): Passive Ammonia SCR System for Lean-burn SIDI Engines. *SAE journal,* Vol. 1, No. 1, 2010, pp. 99-106.

[23] Heeb N.V., Forss A.-M. et al. *Three-Way Catalyst-Induced Formation Of Ammonia - Velocity And Acceleration Dependent Emission Factors,* Atmospheric Environment, Vol 40, 2006, pp. 5986-5997.

[24] Heeb N.V., Saxer C.J. et al. *Correlation of hydrogen, ammonia and nitrogen monoxide (nitric oxide) emissions of gasoline-fueled Euro-3 passenger cars at transient driving.* Atmospheric Environment, Vol 40, 2006, pp. 3750-3763.

[25] Introduction to Fourier Transform Infrared Spectrometry P/N 169-707500 2/01
mmrc.caltech.edu/FTIR/FTIRintro.pdf (18 February 2011)

Appendix A - Calculations

Exhaust mass flow [g/s]:

$$\dot{m}_{exh} = \dot{m}_{fuel}(1 + 14.7 * \lambda) \tag{19}$$

Stored NH_3 [g]:

$$m_{NH_3} = \dot{m}_{exh} * \frac{M_{NH_3}}{M_{exh}}(NH_{3_{pre,ppm}} - NH_{3_{post,ppm}}) \tag{20}$$

Reduced NO [g]:

$$m_{NO} = \dot{m}_{exh} * \frac{M_{NO}}{M_{exh}}(NO_{pre,ppm} - NO_{post,ppm}) \tag{21}$$

NO_x reduction efficiency [%]:

$$\eta_{NOx} = \left(\frac{NO_{x_{pre}} - NO_{x_{post}}}{NO_{x_{pre}}}\right) * 100 \tag{22}$$

Molar mass ratio [n_{NH3}/n_{NO}]:

$$\frac{m_{NH_3} * M_{NO}}{m_{NO} * M_{NH_3}} \tag{23}$$